UNIVERSIDADE FEDERAL DE PERNAMBUCO
CENTRO DE TECNOLOGIA E GEOCIÊNCIAS
DEPARTAMENTO DE ELETRÔNICA E SISTEMAS
PROGRAMA DE PÓS-GRADUAÇÃO EM ENGENHARIA ELÉTRICA

GHULAM ABBAS

A PLASMONIC STUDY OF ELECTRICAL FIELD ENHANCEMENT AND NANOCIRCUIT THEORY OVER NANOPARTICLES AND NANOSLITS

Recife
2019

GHULAM ABBAS

A PLASMONIC STUDY OF ELECTRICAL FIELD ENHANCEMENT AND NANOCIRCUIT THEORY OVER NANOPARTICLES AND NANOSLITS

Thesis submitted to the Graduate Program in Electrical Engineering of the Federal University of Pernambuco, as a partial requirement for obtaining the title of PhD in Electrical Engineering.

Concentration Area: Photonics.

Advisor: Prof. Dr. Emery Cleiton Cabral Correia Lins.

Recife

2019

Catalogação na fonte
Bibliotecária Margareth Malta, CRB-4 / 1198

A122p Abbas, Ghulam.
A plasmonic study of electrical field enhancement and nanocircuit theory over nanoparticles and nanoslits / Ghulam Abbas. - 2019.
80 folhas, il., gráfs., tabs.

Orientador: Prof. Emery Cleiton Cabral Correia Lins.

Tese (Doutorado) – Universidade Federal de Pernambuco. CTG. Programa de Pós-Graduação em Engenharia Elétrica, 2019.
Inclui Referências e Apêndice.

1. Engenharia Elétrica. 2. Amplificação de campo. 3. Circuitos equivalentes. 4. Propriedades óticas. I. Lins, Emery Cleiton Cabral Correia. (Orientador). II. Título.

UFPE

621.3 CDD (22. ed.) BCTG/2019-460

GHULAM ABBAS

"A PLASMONIC STUDY OF ELECTRICAL FIELD ENHANCEMENT AND NANOCIRCUIT THEORY OVER NANOPARTICLES AND NANOSLITS"

Tese apresentada ao Programa de Pós-Graduação em Engenharia Elétrica da Universidade Federal de Pernambuco, como requisito parcial para a obtenção do título de Doutora em Engenharia Elétrica.

Aprovada em: 27/09/2019

BANCA EXAMINADORA

_____

Prof. Dr. Emery Cleiton Cabral Correia Lins
(Orientador e Examinador Interno)
Universidade Federal de Pernambuco

_____

Prof. Dr. Frederico Dias Nunes
(Examinador Interno)
Universidade Federal de Pernambuco

_____

Profa. Dra. Beate Saegesser Santos
(Examinador Externo)
Universidade Federal de Pernambuco

_____

Prof. Dr. Fernando José Ribeiro Sales
(Examinador Externo)
Universidade Federal de Pernambuco

_____

Profa. Dra. Patricia Silva Lessa
(Examinador Externo)
Universidade Federal de Pernambuco

This work is dedicated to my mother
Maimona Bibi

ACKNOWLEDGEMENTS

Up and above everything else, all praises to the ALMIGHTY ALLAH alone, the Omnipotent, the Omnipresent, the most merciful and most compassionate.

I take this opportunity to record my deep sense of gratitude to my worthy supervisor Dr. Emery Cleiton Cabral Correia Lins, co-supervisors Dr. Frederico Dias Nunes, and Dr. Beate Saegesser Santos for their constant efforts, support and providing me this plate form to work on this topic. I am really thank full to them for encouragement, useful suggestions and help in the completion and presentation of this thesis.

I am thankful to my friends Thiago Campos and Cláudio Henrique Rodrigues da Silva for their technical sport during this work and also I would like to say thanks to my lab fellows, Marcel Bezerra , Lucas Gallindo Costa, H Zeeshan Mahmood, Maria Yaseen, Maryam Liaqat and Marlon Silva Ferreira for helping me during my work. I feel my proud privilege to mention the feelings of obligations toward my dearest mother, Maimona Bibi, and father, Zafar Khan, whose encouragement and continuous moral as well as financial support for me to reach this destination. My efforts brought fruit because of their prayers. I feel great pleasure to put on my gratitude to my loving brothers Ghulam Jillani, Farooq Ahmed and Muhammad Waqas for their love, respect, and encouragement throughout my life. Special thanks to my beloved wife for taking care of me for 3 years and my daughter for being a reason of my pleasures during last 2 years.

I would like to say thanks to CAPES for financial support.

Ghulam Abbas

ABSTRACT

We begin with the electromagnetic field propagation through nano slit composed of different materials. Field enhancement, plasmonic characteristics and power flow are discussed. An equivalent circuit that can model the nano slit and surrounding medium is purposed. The different combinations used in the slab include, gold-gold, silver-gold and silver-silver. It is assumed that the nano slit is placed in free space. This study focus on the behavior of electromagnetic field at the surfaces. Further, different types of nanocavities are introduced at the entrance of nanoslit to enhance the power flow and electric field. An excellent response is observed to obtain the required goals and new method to build a nanoslit is presented. Next we consider spherical nanoparticles, that were prepared in lab and also analyzed using COMSOL Multiphysics simulations. The comparison between theoretical and experimental results is presented. Nanospheres with and without coating are considered to study the interaction of electromagnetic field with these particles. The nano particles consist of silver or gold and coating layer of SiO_2 or Al_2O_3 are considered. For the case of nanosphere it is assumed that the surrounding medium is water. Using optical properties and parameter values an equivalent circuit for nanosphere is also modeled. In the next step, we focus on nano ellipsoids placed in free space composed of different materials, we analyze the nano ellipsoids and design corresponding equivalent circuit. We consider that the nanoellipsoid consist of silver or gold and the coating layer consist of SiO_2 or Al_2O_3, similarly as we did in the case of nanosphere. Finally, using seed based approach, silver nanoprisms are fabricated and their optical properties are studied. The experimental and simulation results are obtain to compare the response of nanoprism composed of silver and gold. Based on optical properties and using modeling parameters the values of nanocomponents are calculated. The effect of size shape and surrounding medium are discussed by using different types of nanoparticles. Ag and Au NPs were characterized using Uv-Vis, and SEM. The spectra was recorded on Thermo Scientific Evolution 600S spectrophotometer.

Keywords: Field enhancement. Equivalent circuit. Optical properties.

RESUMO

Nós começamos com a propagação de campo eletromagnético por fendas compostas de diferentes materiais. Aumento do campo, características plasmônicas e fluxo de potencia são discutidos. É proposto um circuito equivalente que pode modelar a nanofenda e o meio. As diferentes combinações de materiais utilizados na fenda são ouro-ouro, ouro-prata e prata-prata. É assumido que a nanofenda é posicionada no espaço livre. Esse estudo foca no comportamento do campo eletromagnético nas superfícies. Adicionalmente, diferentes tipos de nanocavidades são introduzidas na entrada da nanofenda para melhora do fluxo de potência e campo elétrico. Uma boa resposta foi observada e foi apresentado um novo método de construção de nanofendas. Em seguida, são consideradas nanoparticulas esféricas, que foram preparadas em laboratório e analisadas utilizando simulações no COMSOL Multiphysics. É apresentada uma comparação entre os resultados teóricos e experimentais. São consideradas nanoesferas com e sem revestimento, e são analisadas a sua interação com campos eletromagnéticos. As nanopoarticulas consistem de ouro ou prata e uma camada de revestimento de SiO_2 ou Al_2O_3. Para o caso da nanoesfera é considerado um meio composto por água. Também, é modelado um circuito equivalente para nanoesfera utilizando propriedades óticas. No próximo passo são analisados nanoelipsoides compostos de diferentes materiais posicionados no espaço livre, e é elaborado o seu circuito equivalente. É considerado que a nanoelipsoide é composto por ouro ou prata, e contém um revestimento de SiO_2 ou Al_2O_3. São fabricados nanoprismas utilizando método baseado em sementes, e são analisados suas propriedades óticas. Os resultados experimentais e simulados são utilizados para comparar os nanoprismas compostos de prata e de ouro. Os valores dos nanocomponentes são calculados utilizando as propriedades óticas e os paramentros de modelamento. O efeito do formato, tamanho e meio são discutidos utilizando diferentes tipos de nanoparticulas. Ag e Au NPs são caracterizados utilizando Uv-Vis e SEM. O espectro foi capturado utilizando o espectrômetro Evolution 600S, da Thermo Scientific.

Palavras-chave: Amplificação de campo. Circuitos equivalentes. Propriedades óticas.

LIST OF FIGURES

LIST OF ABBREVIATIONS

ω_p	Plasma frequency
ε	Permittivity
μ	Permeability
SPR	Surface Plasmon Resonance
SEM	Scanning Electron Microscopy
TEM	Transmission Electron Microscopy
SiO_2	Silicon Dioxide
Al_2O_3	Aluminum Oxide
Ag-NPs	Silver Nanoparticles
Au-NPs	Gold Nanoparticles
$AgNO_3$	Silver Nitrate
TSC	Trissodium Citrate
PSSS	Sodium Poly 4-Styrene Sulfonate
$HAuCl_4$	Hydrogen Tetrachloroaurate
$NaBH_4$	Sodium borohydride
R	Resistor
C	Capacitor
L	Inductor
V_{th}	Thevenin voltage
Z_{th}	Thevenin resistance
FEM	Finite Element Method

CONTENTS

1 INTRODUCTION

In this chapter we will introduce the concept of plasmonics, nanocircuits and the objectives of our study. We will explain how the phenomena of light mater interaction occurs and its significance.

1.1 Introduction

Plasmonics forms a major part of the fascinating field of nanophotonics, which explores how electromagnetic fields can be confined over dimensions on the order of or smaller than the wavelength. [(1)] Interaction process between electromagnetic radiation and conduction electrons in small metallic nanostructures or at metallic interfaces, is the base of an enhanced optical near field of sub-wavelength dimension. Research in this area demonstrates that nanoparticles can offer an unusual phenomenon with practical applications in many areas. [(1)]

Using Maxwell's equations, the plasmon resonances of nanoparticles can be investigated. [(2)] The permittivity of the metals varies with wavelength because they exhibit frequency dispersion. At optical frequency, metals like silver and gold may have negative permittivity. The interaction of the electromagnetic field with the conduction electrons is the underlying microscopic mechanism that leads towards this negative value of permittivity. For specific negative values of the permittivity, which depend on the shape and size of the particle, an external electromagnetic field can produce a resonantly enhanced polarization that can lead to large electromagnetic fields near the particle. These distinct resonances are known as plasmon resonances or the surface polariton modes of the particle.

Almost for last one hundred years, the optical properties of particles small enough as compare to the operating wavelength have been the point of interest for researchers. Particularly the optical properties of small metallic nanoparticles have gained particular attention. [(3)] The electric field near the surface of the particle is enhanced at frequencies close to the particle plasmon resonance. Quite large values of enhanced field as compare to the incident field have observed in the literature and have been used to enhance a variety of linear and nonlinear optical processes occurring just outside the particle surface. [(4-9)]

Experiments have shown that molecules located within a wavelength of a metal surface can decay, by means of the optical near field, by directly exciting the propagating optical-frequency surface-plasmon mode of the metal–dielectric interface. This direct surface-wave excitation is known to be an important energy-transfer process near metal surfaces, one with

an efficiency that exceeds 90 % under the best conditions. [10] This phenomenon has been used successfully to demonstrate spectacular enhancement of sensitivity in fluorescence measurements [11] and in Raman sensing. [12] This phenomenon has also been described as a method in potential applications in various optical devices, in detectors [13] and to increase the efficiency of solar cells. [14]

Due to involvement and efforts of a large community of theorists in the field of nano-plasmonics, in addition to these impressive experimental results, a better picture of understanding the local field enhancement has been gradually emerged. It has become clear that the enhancement is the largest in the so-called "hot-spots" [12-20] occurring when the metal is structured in a rather sophisticated way with small gaps.

We must focus on the most important parameter maximum enhancement of field to conduct this study as maximum enhancement is limited by the metal losses. A single metal nanoparticle [19] with simple smooth shape (sphere, ellipsoid, or nano-rod) cannot provide the electric field enhancement larger than the Q-factor of the metal, where the Q factor is the ratio of real and imaginary parts of dielectric function of the metal, and as reported in [20] it is less than a factor of 10-20 in the visible and near infrared regions.

But more significant enhancement can occur in the intricately structured and arranged nanoparticles when the field gradually couples from the larger particles or regions serving as antennae into the smaller regions that serve as field-concentrating hot spots. [21] It has been suggested by Stockman [22] that sequential coupling of energy from larger to smaller particles can result in high degree of field concentration.

For metals like silver and gold, the plasma frequency ω_p of the electron gas lies in the optical range. This provides very strong interaction of these metals with light and leads to a highly dispersive dielectric function at optical frequencies. [19] In particular, the real part of the permittivity ε (ω) changes sign when the illumination frequency ω reaches close to ω_p. For particles smaller than the skin depth, this microscopic interaction can result in a resonance of the entire particle, known as a plasmon resonance or a surface mode of the particle. [20] It is well known that a spherical nanoparticle has its single resonance frequency when $Re\,[\varepsilon] = -2\varepsilon_0$.

The surface plasmon resonances are found somewhere in the visible to near-infrared spectral region, depending on the particle shape, the environment and the metal [21], in this work we will study these parameters to complete the results.
Smartly engineered structure parameters of nanoparticles are the key components that are used to control the functionalities of plasmonic nanodevices. In conventional circuit theory, at microwave and radio frequencies, lumped circuit elements, i.e., resistor, inductor and capacitor are effectively and flexibly used to design the basic building blocks for designing complex micro-electronic devices.

The conventional circuits in the lower frequency domains (such as in the RF and lower frequency range) indeed involve elements that are much smaller than the wavelength of operation, and the circuit theory may be regarded as the ‘‘approximation’’ to the Maxwell equations in the limit of such small sizes. It should be pointed out that a mere scaling of the circuit component concepts conventionally used at lower frequencies may not work at frequencies beyond the far infrared, since conducting materials (e.g., metals) behave differently at these higher frequencies. In [23], using quasistatic approximation approach the concept of the circuit elements including nanoinductors, nanocapacitors and nanoresistors is presented. Such concepts may be extended to more arbitrary configurations of nanoparticles. As in this work based on this knowledge of nanocircuits, we will present the equivalent circuit for nanoslit, nanosphere and nanoellipsoid.

In electronics, basic functions are synthesized using ‘lumped’ circuit elements and more different operations can be performed by combining these circuit elements in specific series or parallel ways. To perform these operations in infrared or visible domain the optical analogy requirements cannot be achieved by simply reducing the basic unit size of the circuit element from micrometer to nanometer scale. The fact that does not allow to adopt this analogy is material dispersion which may be vital for some cases. Metals such as silver, gold, copper and aluminum are highly conductive materials at radio frequencies and microwaves.
At optical frequencies these metals behave differently, instead of usual conductivity, these metals exhibit plasmonic resonance. When the real part of permittivity is negative, optical signals coupling with collective oscillation of conduction electrons dominate at the surface of these metals. At optical wavelengths, the conduction current remains no longer the dominant

current circulating through lumped optical elements. As a result, the traditional circuit theory and its methodology lose their functionality in optical frequency domain.

Engheta et al. proposed the concept of 'metatronics' [23-24] that bridges the gap between high frequency nanodevice design and conventional low frequency circuitry design. By properly arranging and designing non-plasmonic and/or plasmonic nanoparticles it is possible to realize the lumped-circuit-like elements at optical frequencies. 'Metatronics" has simple framework that is based on one Maxwell equation

$$\nabla \times \boldsymbol{H} = -j\omega \boldsymbol{D} + \boldsymbol{J}_c \ldots\ldots\ldots\ldots\ldots (1.1)$$

Equation (1.1) has two term on its right side, first, displacement current and the second is conduction current. As the dispersion of material plays critical role at optical wavelength, and the conduction current do not dominate any more that originally dominates at low frequencies. In this situation, the displacement current can be considered as flowing optical current. So this change in role of dominant current requires to rebuild the formulae to calculate the lumped impedance of nanoparticles at optical frequencies. The optical impedance, which is intrinsic property of nanoparticles, is similar to the electrical counterpart ($Z = V/I$) and it is independent of the surrounding medium. [25]

In circuit theory, the lumped elements are completely isolated from the external environment and their interaction with the circuit depends on their connection with the rest of the circuit. In contrast, in the case of equivalent circuits, external and fringing fields play dominant roles in the interaction of nanoparticles with their surrounding environment and neighboring particles, so based on the orientation of the external applied field the same connection may be presented as series or parallel connection. This characteristic provides additional and important degree of freedom in the designing of optical nanocircuit. Recently [25, 26], it is experimentally verified that it is possible to alter the functionality by reconfiguring the circuit response by changing the polarization and orientation of incident field. By applying these function it is possible to achieve different features by using same circuit that was not possible by using conventional electric circuits. For example, for a circuit when set to operate in as series connect acting as band stop filter may behave as band pass filter when the configuration is changed from series to parallel by changing the polarization of incident field.

Silver nanoparticles of different shapes are of considerable interest in nanotechnology. The collective oscillation of the conduction electrons in resonance with particular frequencies of incident light leads to an extinction known as surface plasmon resonance is major

characteristic of silver nanoparticles that provides new directions to investigate these nanoparticles. [27-28] Shape, size and refractive index of the nanoparticle and refractive index of the surrounding medium are the key factors on which the spectral position of the resonance highly depends. At the surface plasmon resonance (SPR) of a metal nanoparticle, the electric field intensity at the interface between metal nanoparticle and surrounding medium is enhanced strongly as compare to the applied field that is the key and most interesting property of highly shaped nanoparticles. [27, 29] Two potential applications of this field enhancement are Surface Enhanced Raman Spectroscopy (SERS) and Surface Enhanced Fluorescence (SEF). [31-34] These applications of are the driving force for the development of synthetic approaches that provide high degree of control on the final nanoparticle morphologies. The in-plane dipole surface plasmon resonance can be tuned across the entire visible spectrum starting from 400 nm to the near infrared. [35-39]

In this work we will prepare silver and gold nanospheres to study the optical properties and will compare the experimental results with the results obtain by performing simulations. Both types of nanospheres will be prepared based on thermal synthesis. For the production of silver nanoprisms the syntheses process can be divided in to two categories fist one is photochemical that is based on plasmon-driven synthesis [38, 40] and second is thermal. [32, 41] Photochemical synthesis produces the high quality samples but this approach involves few days to prepare a sample. On the other hand, thermal approaches are much quicker but often they produce samples with a range of sizes and shapes. [42-44]

The method we used for synthesis of silver nanoprism in this work is seed-based thermal procedure that selectively produces silver nanoprisms in a reproducible and rapid manner. This method can be performed under mild conditions (room temperature and water solvent). Without applying any significant variation in the thickness, the spectral position of surface plasmon resonance can be tuned by controlling the size of nanoprisms. The size of nanoprisms can be changed by adjusting the number of seeds in the growth mixture.

To prepare high quality samples one key ingredient is poly (sodium styrenesulphonate) (PSSS), that plays the role of stabilizer in the seed production step. Missing of this stabilizer or adding it to seed solution after seed production can cause a diversity of nanoparticle sizes and shapes. This shows that PSSS does not play simple role in shape directing by preferential adsorption to certain crystal faces during the growth but it has strong influence on the defect structure of the seeds and preference for seed that undergo their structural chage, i.e., sphere

to nanoprism. Characterization of the nanoprisms produced by this method can be performed using SEM or TEM analysis and to explore the relationship between nanoparticle dimensions and the position of surface plasmon resonance using this method samples with different dimensions can be prepared.

In chapter 2, we will present the review of literature on nano slit, nanosphere, nanoellipsoid and nanoprism.

In chapter 3, an equivalent circuit that can model the nanoslit and surrounding medium will be purposed. We will develop an equivalent circuit for nanoslit and will study the phenomenon of field enhancement inside the nanoslit, plasmonic characteristics and Fabry-Perot. The different combinations will be used in the slab include, gold-gold, silver-gold and silver-silver. This study will focus on the behavior of electromagnetic field at the surfaces. We will also describe spherical nanoparticles with and without coating to study the interaction of electromagnetic field with these particles. The basic equivalent circuit for different types of materials will also be discussed. The preparation of silver and gold nanosphere will be discussed in details. The nano particles consist of silver or gold or aluminum and coating layer consist of silicon dioxide (SiO_2) or aluminum oxide(Al_2O_3). Using same materials we assumed for core and shell for nanospheres, we will discuss the optical properties of nanoellipsoids. The objective of this study is to observe the effect of shape on the optical properties of nano particles and to compute the corresponding nano circuit elements. We will discuss the optical properties of nanoprism and the preparation of silver nanoprism in the lab and conclude how the change in shape of nanoparticles effect the optical properties of these nanoparticles.

In chapter 4, the response of nanoslit composed of different types of materials will be discussed, further to increase the power flow in different types of nanoslit, nanocavities will be introduced at the entrance of nanoslit and the corresponding effects will be explained. Silver and gold nanospheres will be prepared in lab and their structural and optical properties will be studied. We will present the results and discussion for nanoslit, nanosphere, nanoellipsoid and nanoprism. We will analyze optical properties and field enhancement using different sizes of nanoellipsoids and will design corresponding equivalent circuit. Using seed based approach it will be shown how we can prepare silver nanoprisms from silver nanospheres.

In chapter 5, we will conclude the results and discussions.

2 LITERATURE REVIEW

In chapter 1, we introduced the concept of light mater interaction and the importance of equivalent circuits. In this chapter, we briefly review the literature about nanoslits, nanospheres, nanoellipsoids and nanoprisms.

2.1 Review of Literature

Basic equivalent circuits for different type of nanostructures, i.e., nanoslit [45], nanosphere [46] and nanoellipsoide [47] are presented in the literature. Based on basic circuit elements, i.e., nanoinductors, nanocapacitors, and nanoresistors, the concept of circuit nanoelements using plasmonic and nonplasmonic nanoparticles was presented in the optical domain. [46] Based on characteristic impedance model a method to analyze elementary subwavelength structures interacting with light was presented. [45] These nanoelements may have applications in different areas such as nano-optics, biophotonics, optical information, molecular signaling and biological circuits. [46]

As described by Ghaemi et al. [48] how extraordinary optical transmission can be achieved using sub-wavelength hole arrays. In last two decades transmission of light from nano slit has been an interesting topic for researchers where they used array of slits to study the field enhancement [49-51], transmission resonances [52], transmission and focusing properties [53] of nano slits. It was also described that [54] how optical transmission can be enhanced by using multiple paths. Y. Takakura [55] explained the optical response in a narrow slit in a thick metallic screen and observed Fabry-Perot-like behavior during the interaction of TM-polarized waves with a subwavelength thick metallic slit. In the petahertz domain high frequency response of subwavelength-structured metals was discussed in details. [56]

A bulk material consists of constant physical properties that do not depend up the shape or size of material. On the other hand, at nanoscale, morphology plays key role to change the physical, chemical and biological properties of particles. For example at nanoscale, nanosilver possesses the antibacterial character and becomes an odor eater and at nanoscale the melting point of gold decreases from 1064^0 C to 100^0 C. [57]

When nanosphere with radius very less as compare to the operating wavelength of light is exposed to light, free electrons of nanosphere interact with photon energy and they produce subwaves and conducting electrons in oscillating mode offering localized surface plasmonic resonance (LSPR). LSPR adds the benefits of enhanced UV-Vis absorption, enhanced local

electric and molecular polarization effects. [58] Core applications of these nanoparticles include medicine, optics, renewable energies, inks, microelectronics, medical imaging, and biomedical devices. [59–61]

Silver nanoparticles (Ag-NPs) are most popular due to their unique chemical, physical and biological properties. [62] As compare to the other noble metals Ag-NPs are non-toxic, high electric conductivity, small loss of the optical frequency during the surface plasmon propagation and low cost, wide absorption of visible and far IR region of the light, surface-enhanced Raman scattering and nonlinear optical behavior. [63] Moreover, they exhibit a broad spectrum of high antimicrobial activity, attracting the scientists and technologists with much interest to develop nanosilver-based disinfectant products. [64]

Based on size dependent electromagnetic and optical properties, silver nanoparticles (NPs) have applications in optics, electromagnetics, water treatment and antibacterial agents in biotechnology and bioengineering among many others. [65-66] Silver NPs are being used in many technologies that take advantage of their-optical and antibacterial properties. The use of silver NPs in biosensors to efficiently enhance optical spectroscopy, i.e., surface enhanced Raman scattering (SERS) is other example. [67]

Since ancient times optical properties of colloidal gold nanoparticles have been used in particular for staining glass. It is possible to synthesize gold nanoparticles of diameters ranging from few nanometers up to several hundred nanometers. During typical syntheses process, reducing agent is used to reduce gold salts leading to the nucleation of Au ions to nanoparticles. Stabilizing agent, it could be adsorbed or chemically bound to the surface of the Au nanoparticles, is used. Typically, stabilizing agent is charged, so that the equally charged nanoparticles repel each other and as a result they remain stable. Citric acid is very commonly used to reduce gold salt. [68]

Interaction of gold nanoparticles with light is the base for most prominent detection techniques. [69] Gold nanoparticles can strongly absorb and scatter light. When they absorb light, the light energy excites the free electrons present in Au nanoparticles to a collective oscillation, known as surface plasmon. [70] At plasmon resonance frequency the absorption cross-section is very high. This light absorption leads to heating of Au particles. In several ways, interaction of Au nanoparticles with light is used for the visualization of nanoparticles. Au particles are used for labelling with different colors as the color of light scattered by these particles depends on their size and shape. [71]

The scattering cross-section for small particles decreases rapidly whereas the absorption cross-section decreases less. This absorbed light heats the particles and subsequently these heated particles transport this heat to their surrounding environment. Depending on the application, different microscopy techniques are used to detect Au particles include, dark field microscopy, scanning electron microscopy (SEM) and transmission electron microscopy (TEM) among others. [72]

In general, Raman signals are quite weak, but this Raman scattering dramatically enhanced if the molecules of subject under exam are placed closer to the gold surface as for example small gold nanoparticles. This effect is called surface-enhanced Raman scattering (SERS). Plasmon resonance of these nanoparticles produces enhancement of the electric field in close proximity to these nanoparticles as compared to the field of incident light. [73] Very reliable intrinsic property of gold nanoparticles at their resonance frequency can be used for sensing applications. [74]

In certain noble metals such as silver and gold, it is well known that in the ultraviolet or visible regimes plasma frequency does exist and they behave as plasmonic materials and the real part of their permittivity is negative. [75] As conducting materials (e.g., silver and gold) behave differently at higher frequencies, the circuit component concepts conventionally used at lower frequencies may not work accordingly beyond far infrared frequencies. Engheta et al [76] presented the concept of synthesizing circuit elements in the optical regime.

On metal nanoparticles, we can excite surface plasmons when illuminated at a specific frequency. So it is possible to consider these oscillations in terms of electric circuits and can be described in the form of circuit elements such as resistor '*R'*, capacitor '*C'* and inductor '*L*'. Engheta et al. explained the correspondence between metal nanoparticles and circuit elements in terms of electric permittivities. [76-77] Nunes et al has shown that optical surface waves at planar structures may be analyzed as electric circuits, being described as transmission lines or condensed circuits. [78-79]

Nanoparticle structures supporting localized surface plasmons can be modeled as standard circuits composed of resistance, capacitance and inductance. At optical frequencies, when the real part of electric permittivity is positive the equivalent circuit presents capacitive behavior and being inductive when negative value is the case, as shown by metals for characteristic range of frequencies.

For dielectric surrounding medium, where a nanostructure is present, its equivalent circuit corresponds to a capacitive circuit. The imaginary part of permittivity requires a circuit resistive behavior, for describing dissipative effect, for both nanoparticle and enviroment. This corresponds to metal ohmic losses being represented as resistance. [76]

The plasmon circuit model provides a way to design optical elements based localized surface plasmons. This method gives a new approach to understand plasmonics behavior of nanoparticles and to manipulate optical information. [79-82] Before this, interpretation of plasmonics was considered a typical optical phenomenon.

Controlling the shape and size of the nanoparticles can result in changing the positive/negative charge separation and the intensity and frequency of localized surface plasmon resonance (LSPR) can be tailored in visible and the infrared region. [83] For nanoparticles with different symmetry axis, more than one plasmonic modes are observed [84] and ellipsoidal nanoparticles are the most interesting nanostructures among this kind of nanpparticles. Due to 3-fold symmetry, nanoellisoidal particles exhibit both longitudinal and transverse plasmon modes. The effect of length distribution on the extinction coefficient of gold oblate and prolate spheroidal nanoparticles arranged in two dimensional arrays has been studied experimentally [85], and the linear dependency of the peak position of the plasmonic mode with respect to the length of the corresponding principal axis was observed. To study plasmonic modes of the ellipsoidal particle quasistatic approximation was used to find an analytical expression for the plasmon frequency. [86] The optical properties of an oriented isolated nanoellipsoidal particle both for the gold (Au) and silver (Ag) cases were studied [87] and concluded that the optical response of the metallic ellipsoidal nanoparticle is quite specific when compared to other nanoparticle morphologies due to the possibility of three different LSPR modes. Based on optical properties of nanoellipsoidal particles different applications using nanoellipsoidal particles are presented. [88-89] The concept of equivalent nanocircuits for nanoellipsoids is also discussed in [47] and the roots of the theoretical models of the nanotechnoscience in the electric circuit theory are explained. [90]

Interpretation of light interaction with plasmonic nanostructures in terms of circuit models has been discussed in literature. [1] Nanoparticles with size of nanometers are of particular interest in the new technological developments. The major characteristic of these nanoparticles is their large surface area to volume ratio for surface study, for example surface enhanced Raman scattering (SERS) is the best known example up to date. [4-7] Gold and silver nanoparticles

being non-reactive and non-toxic are used as the metallic probs. Sliver provides higher magnification on the other hand gold colloid solution is highly stable. Due to relatively sharp spectrum of surface plasmon, silver nanoparticles produce high local electric filed when exposed to light at resonance wavelength.

3 MATERIALS AND METHODS

In this chapter we will explain how the equivalent circuits for nanoslit, nanosphere and nanoellipsoid can be designed. It is shown that how depending upon the properties of materials corresponding electric nanocomponents can be designed. The motivation behind this work is that in future how we can reduce the size of optics devices. This chapter presents the materials required for the preparation of different types of nanoparticles and techniques to visualize the structural and optical properties. The other objective of this chapter is to explain the experimental and simulation techniques that are used to study optical properties of different particles.

3.1 Equivalent circuit for nanoslit

The motivation behind investigating this kind of equivalent circuits is their scalar form that reduces the complexity of design. We discuss how the response of nanoslit, when it is exposed to light can be represented as an equivalent circuit. The electromagnetic coupling between nanoslits can be presented as arrays of *RLC* circuits. Ohmic losses can be represented as resistance of the circuit and permittivity of dielectric as inductance *L* and negative permittivity of the metal as capacitance *C*, respectively. (3)

Figure 1 - Nanoslit with thickness *t* and width *w* placed in free space. Transverse magnetic (TM) mode polarized plane wave incident normal to the top surface.

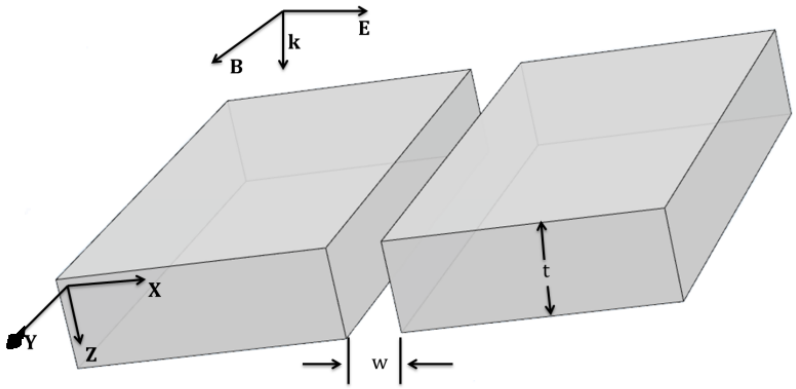

Source: The Author, 2019.

Equivalent circuit of the nanoslit and its surrounding is shown in figure 1. We assume that a subwavelength nanoslit of width *w* and thickness *t* is milled into a subwavelength metal layer. Dielectric material above, inside and below the slit is same (dielectric). However metal

surface changes in different cases as we have assumed three different cases, i.e., gold-gold, silver-silver and silver-gold surface. In the case of silver-gold slit the impedance of metal on both sides of slit is different. This difference of impedance on both sides of slit can be interesting tool as discussed in chapter 4. The width and thickness of slit are of subwavelength.

Figure 2(a) shows a schematic of the corresponding equivalent circuit for nanoslit and its surrounding medium and figure 2(b) represents the impedance model of figure 1. When Transverse Magnetic (TM) polarized plane wave on the top of the slit interacts with the dielectric metal interface, a standing wave is generated. The magnetic field component of the wave is adjacent to the surface and penetrates to the skin depth within a real metal. This time-harmonically oscillating magnetic field induces currents and voltages on the top surface, within the skin depth and on the slit walls. [11] The equivalent circuit in figure 2(a) consists of two symmetrical voltage sources V_1 and V_2, these sources are impact of incident wave. The currents passing in the slit generate the inductance *L*. Currents on the walls of slit generate capacitance *C* and internal resistance of the material is mentioned as *R*. The expressions for Thevenin voltage V_{th} and Thevenin resistance Z_{th} of circuit shown in figure 2(b) are calculated in equation (3.1) and (3.2). In circuit analysis Laplace transform is used for simple conversions of circuit elements to the S-domain. [1]

Figure 2 – Equivalent circuit model of nanoslit

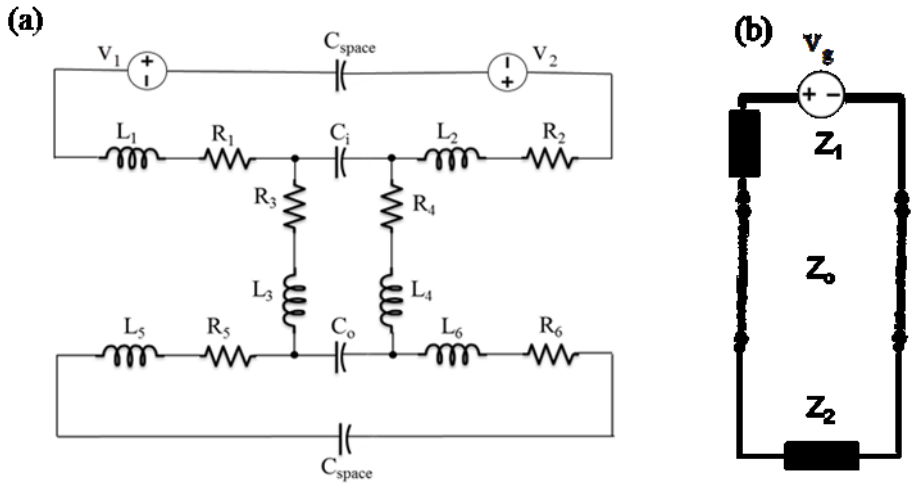

Source: The Author, 2019.
(a) components of equivalent circuit of nanoslit (b) impedance model.

Similar to phasor impedances, circuit elements can be transformed in to impedances using Laplace transform. Using Laplace transform the relation for Thevenin voltage is

$$V_{th} = \frac{\omega_i^2}{[s^2 + (\omega_0^2 + \omega_i^2) + \frac{R}{L}s]} V_g \qquad (3.1)$$

Where ω is angular frequency, $\omega_{0,i}^2 = \frac{1}{LC_{0,i}}$

Similarly the relation for Thevenin resistance can be obtained using Thevenin theorem and Laplace transform as

$$Z_{th} = \frac{\frac{1}{sC_0}\left(s^2 + \omega_i^2 + \frac{R}{L}s\right)}{\left[s^2 + (\omega_0^2 + \omega_i^2) + \frac{R}{L}s\right]} \qquad (3.2)$$

Using impedance approach, we can model the impedance equivalent circuit model as shown in appendix A, it consist of a voltage source V_g followed by impedance Z_{th}, Z_0 is impedance of transmission line and Z_2 is load impedance.

$$Z_2 = \frac{\left(s^2 + \omega_s^2 + \frac{R}{L}s\right)\frac{1}{sC_0}}{\left(s^2 + \omega_s^2 + \frac{R}{L}s\right) + \frac{1}{LC_0}} \qquad (3.3)$$

$$V_0 = \left[\frac{Z_0}{Z_{th} + Z_0}\right]\left[\left(\frac{(1+\Gamma_2)e^{-i\beta h}}{1 - \Gamma_1\Gamma_2 e^{-2i\beta h}}\right)\right]V_{th} \qquad (3.4)$$

3.2 Equivalent circuit for nanosphere

We consider a plasmonic nanosphere (Silver or Gold) with dielectric function $\varepsilon(\omega)$ that is complex quantity as shown in figure 3. The size of sphere is much smaller than the operating wavelength in the vacuum and in the plasmonic material. We consider a monochromatic incident electromagnetic plane wave illuminating the plasmonic nanosphere. The plasmonic nanosphere is placed in lossless, homogeneous, non-dispersive and isotropic media, i.e., free space. The permittivity of the free space is ε_0 and permiability is μ_0. As compare to the wavelength the size of nanosphere is very small, so using well-known time harmonic, quasistatic approach the scattered electromagnetic fields inside of the nanosphere and in the

vicinity can be calculated. This quasistatic approach leads to the following expressions for the fields inside and outside of the nanosphere. [7, 23, 25, 26]

Figure 3 - A basic nanoscale circuit in visible regime for plasmonic nanosphere

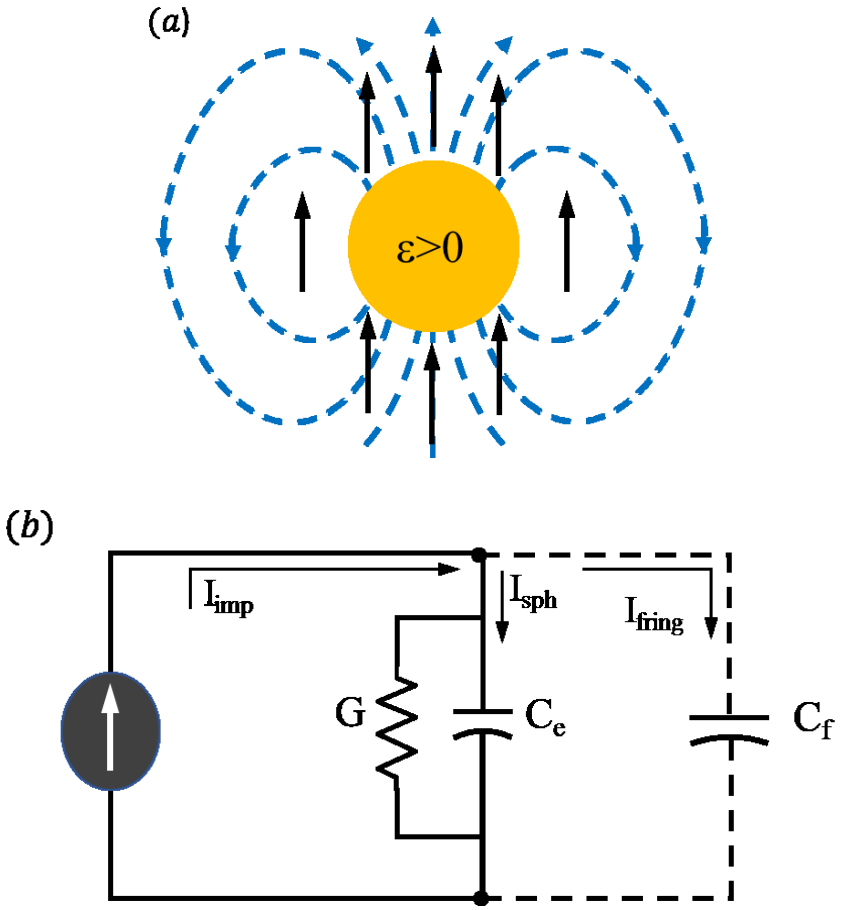

Source: Adopted from the Ref. [7].
Note: (a) nanoplasmonic sphere with $\varepsilon > 0$, which provides a nanocapacitor and a nanoresistor as shown in figure (b).

$$\mathbf{E}_{\text{int}} = 3\varepsilon_0 \mathbf{E}_0 / (\varepsilon + 2\varepsilon_0) \tag{3.5}$$

$$\boldsymbol{E}_{ext} = \boldsymbol{E}_0 + \boldsymbol{E}_{dip} = \boldsymbol{E}_0 + [3\boldsymbol{u}(\boldsymbol{p}.\boldsymbol{u}) - \boldsymbol{p}] / (4\pi\varepsilon_0 r^3) \tag{3.6}$$

Where $$\boldsymbol{p} = 4\pi\varepsilon_0 \boldsymbol{R}^3 (\varepsilon - \varepsilon_0) \boldsymbol{E}_0 / (\varepsilon + 2\varepsilon_0)$$

And $$\boldsymbol{u} = {}^{\boldsymbol{r}}/_{r}$$

Where r is position vector from the center of sphere to the observation point. Boundary conditions at the surface of plasmonic nanosphere show the normal component of displacement current is continuous at the surface:

$$-i\omega(\varepsilon - \varepsilon_0)\boldsymbol{E}_0.\hat{\boldsymbol{n}} = -i\omega\varepsilon_0\boldsymbol{E}_{dip}.\hat{\boldsymbol{n}} + i\omega\varepsilon\boldsymbol{E}_{res}.\hat{\boldsymbol{n}} \qquad (3.7)$$

Where $\hat{\boldsymbol{n}}$ is the local outward unit vector normal to the surface of the nanosphere. In this equation

$$\boldsymbol{E}_{res} \equiv \boldsymbol{E}_{int} - \boldsymbol{E}_0$$

is the residual field internal to the nanosphere when the incident field is subtracted from the total internal field.

3.2.1 Nonmetallic Nanosphere

For this configuration the real part of permittivity is positive so that the impedance is of capacitive nature along with the imaginary part of permittivity acts as resistance of nanosphere as shown in figure 3 (a). As it is always assumed that the outside region has positive permittivity so that the impedance of the outside fringe is always capacitive. Thus the equivalent nanocircuit for a nonplasmonic nanosphere composed of silver or gold can be imagine as shown in the figure 3 (b). In terms of parameters of the nanospheres the equivalent circuit elements can be expressed as follows: [7, 23, 92]

$$C_{sph} = \pi R\mathrm{Re}[\varepsilon] \qquad 3.8(a)$$

$$G_{sph} = \pi\omega R\mathrm{Im}[\varepsilon] \qquad 3.8(b)$$

$$C_{fringe} = 2\pi\omega R\varepsilon_0 \qquad 3.8(c)$$

Where C_{sph} shows the capacitance of sphere, C_{fringe} is capacitance of surrounding medium and G_{sph} is reciprocal of resistance. Since there are two capacitive elements, there is no resonance present in this case a fact that is consistent with the absence of resonance for optical wave interaction with the small nonplasmonic nanosphere. In figure 3 (a) solid black arrows represent the incident electric field, and the thinner field lines together with the blue arrows represent the fringe dipolar electric field from the nanosphere.

3.2.2 Metallic Nanosphere

When the nanosphere is composed of a plasmonic material, such as noble metals, e.g., silver and gold, in the visible or infrared band in this case the real part of permittivity of these metals may have a negative value in these frequency bands as shown in figure 4 (a). So the equivalent impedance of the plasmonic nanosphere can be negatively capacitive for any

frequency for which $\mathrm{Re}[\varepsilon] < 0$. As discussed in [46, 76] this can be interpreted as a positive *effective* ‘‘inductance,’’.

Figure 4 - A basic nanoscale circuit for metallic nanosphere in visible regime

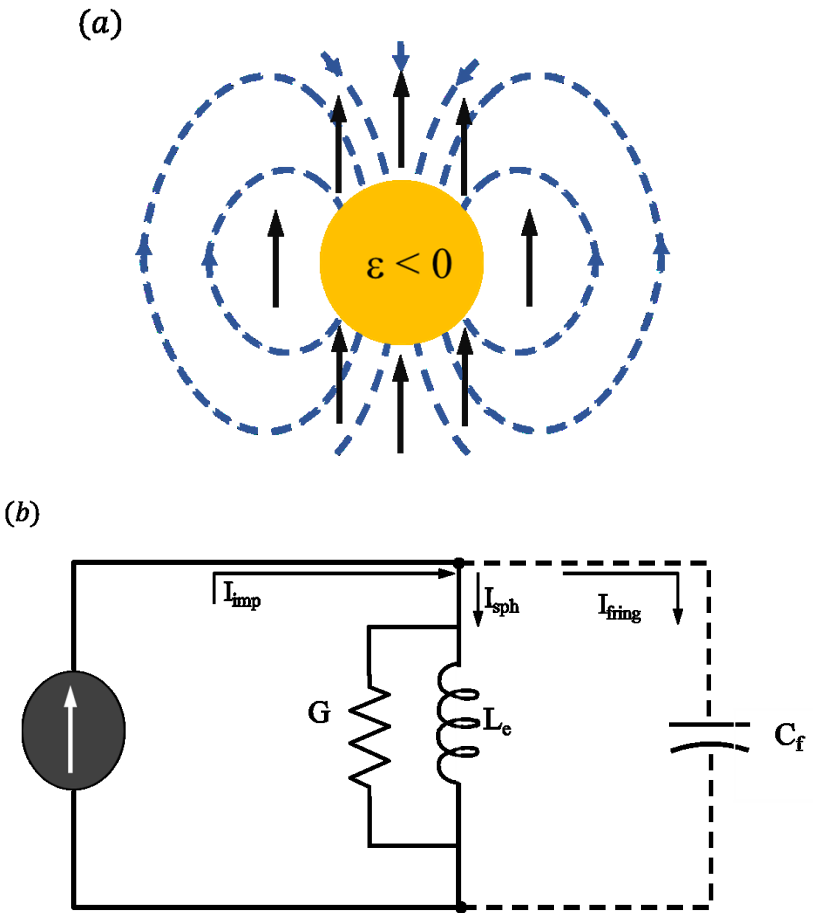

Source: Adopted from Ref. [7].

Note: (a) A nanoplasmonic sphere with $\varepsilon < 0$, which provides a nanoinductor and a nanoresistor as shown in figure (b), solid black arrows represent the incident electric field, and the thinner field lines together with the blue arrows represent the fringe dipolar electric field from the nanosphere.

Therefore, the equivalent circuit for the case of optical wave interaction with a plasmonic nanosphere may be presented as shown in figure 4 (b). Here the inductance of equivalent circuit for the sphere becomes:

$$L_{sph} = (-\omega^2 \pi \mathrm{R}\, Re[\varepsilon'])^{-1} \qquad (3.9)$$

In this case the fringe capacitor is parallel to the inductor as a result the circuit may exhibit resonance, as mentioned in, [52] this resonance corresponds to the plasmonic resonance for the

metallic nanoparticles which interact with the optical wave. The resonance condition for the circuit is

$$L_{sph}C_{sph} = \omega^{-2} \qquad (3.10)$$

requires the well-known condition of plasmonic resonance for a nanosphere

$$Re\,[\varepsilon] = -2\varepsilon_0$$

We conclude from this discussion that a small nanosphere, when excited by an optical signal may behave effectively as a nanocapacitor or a nanoinductor at the optical frequency such that the nanosphere is made of nonplasmonic or plasmonic materials, respectively.

One more importance parameter of any nanocircuit could be nanoresistor. An equivalent nanoresistor may be designed based on the imaginary part of the material permittivity. An effective intrinsic inductance may be modeled by using the plasmonic characteristics of natural noble metals. The value of intrinsic inductance depends on parameters, e.g., shape, size and material contents of the nanostructure.

Nano-optics has been very exciting subject in the nanotechnology during the last decade. The main concentration is on subwavelength optics and applications based on plasmon. [23] In the optical range, magnetic resonant structures and magnetic plasmons have been mainly focused on metallic structures with unavoidable losses and saturation effects inherent to metals. [24, 25] Moreover, it is required that the size must be comparable to the operating wavelength or a fraction of the operating wavelength in order to provide a non-negligible response. The magnetic response is strongly influenced and affected by an intrinsic quadrupolar contribution. This contribution introduces additional impurity of polarization and radiation and additional radiation losses. [26]

One of the most important factor is the enhancement of the electromagnetic field intensities around subwavelength-size metal particles due to the coupling between the incident photons and collective oscillation of free electrons at the metal surface.

3.3 Coated nanosphere

Based on the discussions in pervious sections in this chapter, we can consider a coated nanosphere and develop its equivalent circuit model. We will use silver, gold and aluminum as metal nanoparticles and silicon dioxide(SiO_2), glass and aluminum oxide (Al_2O_3) as

coating materials, as shown in figure 5. Metal nanoparticles and nanoshells consisting of metal shells and dielectric cores are known to enhance incident electromagnetic fields around themselves due to surface plasmons. The field enhancement factors can be calculated for spherical metal nanoparticles and nanoshells in the quasistatic limit using empirical wavelength-dependent dielectric constants.

We will investigate the dependence of the field enhancement factor on various parameters such as metal element, wavelength, surrounding medium, dielectric core material and diameter ratio between the core and the shell.

It also has been known that nanoshells, concentric nanoparticles consisting of a dielectric core and a metallic shell, exhibit attractive features due to the hybridization of the plasmons supported by the nanoscale sphere and a cavity in the surrounding medium. [93-95]

By adjusting the relative core and shell dimensions, we can widely tune the resonance frequency, or the peak wavelength for field enhancement, of a nanoshell, while the optical resonance is essentially a fixed frequency resonance, almost independent of their particle sizes for metal nanospheres. We will apply the quasistatic analysis to find the intensities of electromagnetic fields around subwavelength-size metal nanoparticles and nanoshells. In the following, we extend this nanocircuit concept to the general case of a nanoellipsoid. Such concepts may be extended to more arbitrary configurations of nanoparticles, and may provide methods to model a planar substrate underneath these nanocircuits. We report on the numerical analysis of the local electric field enhancement of silver and gold ellipsoids placed in the free space.

Figure 5 - Schematic configuration of a metal nanoparticle or nanoshell illuminated by plane wave. Where ε_1 represents the permittivity of metalic nanoparticle, ε_2 dielectric coating and ε_3 surrounding medium (free space), respectively.

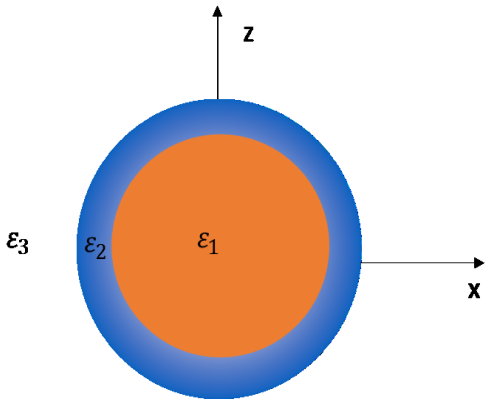

Source: The Author, 2019.

3.4 Equivalent circuit model for nanoellipsoid

This work is organized as follows: we will discuss briefly the basic idea of the equivalent circuit, followed by a presentation of the impedance matching, the corresponding structural parameters, resistor, inductor and capacitor. We consider an ellipsoidal nanoparticle with semi-axes *a*, *b*, and *c* (where *a* > b > *c*).

Figure 6 - An ellipsoidal nanoparticle and its equivalent circuit.

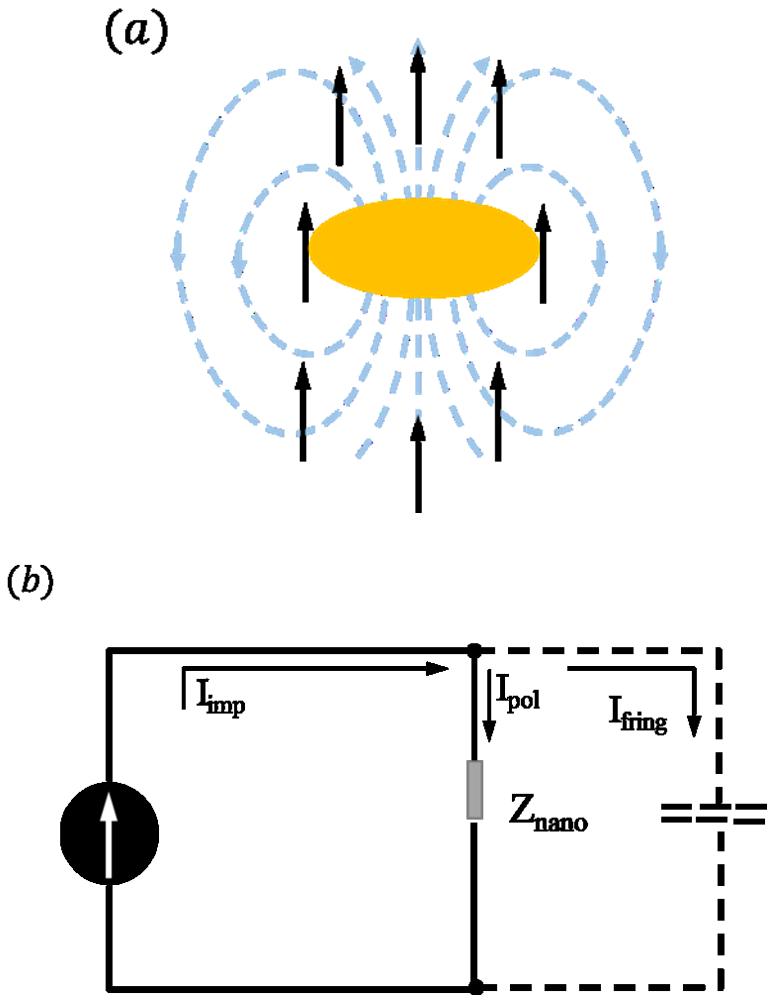

Source: Adopted from the Ref. [47].

Note: (a) An ellipsoidal nanoparticle illuminated by a uniform electric field (b) lumped impedance Z_{nano} excited by the impressed current generator I_{imp} and load with the fringe cacitance associated with its fringe dipolar fields.

The effective impedance of such ellipsoidal nanoparticle excited by a uniform electric field parallel to the *c* axis can be defined as: [47]

$$Z_{nano} = \frac{U(a,b,c)}{-i\omega\varepsilon\pi ab} \qquad (3.11)$$

With

$$U(a,b,c) \equiv \left[\frac{2c\int_{S_{up}}\sqrt{(c^2+\eta)(c^2+\zeta)}\,dS}{\sqrt{(a^2+c^2)(b^2-c^2)}\,S_{up}}\right]$$

Z_{nano} in equation (3.11) is nanoimpedance that can be defined with analogy to the circuit theory as the ratio of the voltage V across the two terminal of the nanoelement and the displacement current I_{pol} flowing through it [47,88]. This impedance is a fixed quantity, depends on the constituent materials of the particle, its geometry and may be on the orientation of the applied field in case if particles having anisotropic polarizability.

Where η and ζ are the transverse coordinates on the ellipsoid in a confocal ellipsoidal reference system and the integral is taken over half of the ellipsoidal surface with area S_{up} [46-47]. In this case, the fringe impedance Z_{fringe} and the impressed current I_{imp} are given by the expressions:

$$Z_{fringe} = \frac{U(a,b,c)}{-i\omega\varepsilon_0\pi ab\,\frac{1-L_z(0)}{L_z(0)}} \qquad (3.12)$$

$$I_{imp} = -i\omega(\varepsilon-\varepsilon_0)\pi abE_0 \qquad (3.13)$$

Where

$$L_z(0) \equiv \frac{abc}{2}\int_0^{\infty}\frac{dq}{(c^2+q)\sqrt{(q+a^2)(q+b^2)(q+c^2)}} \qquad (3.14)$$

Such expressions converge for sphere when $a = b = c$, i.e., in the spherical geometry. Equivalently, the effective circuit elements for a generic nanoellipsoid, its equivalent capacitance $C_{eq,ellipsoid}$, inductance $L_{eq,ellipsoid}$, resistance $G_{eq,ellipsoid}$ and equivalent fringe capacitance $C_{eq,fringe}$ are:

$$C_{eq,ellipsoid} = \frac{\pi ab\,\mathrm{Im}(\varepsilon)}{U(a,b,c)}\ if\ \mathrm{Re}(\varepsilon) > 0 \qquad (3.15\ (a))$$

$$L_{eq,ellipsoid} = \frac{U(a,b,c)}{-\omega^2 \pi ab \,\mathrm{Re}(\varepsilon)} \; if \; \mathrm{Re}(\varepsilon) < 0 \qquad (3.15\ (b))$$

$$G_{eq,ellipsoid} = \frac{\omega \pi ab \,\mathrm{Im}(\varepsilon)}{U(a,b,c)} \qquad (3.15\ (c))$$

$$C_{eq,fringe} = \frac{\varepsilon_0 \pi ab \dfrac{1 - L_z(0)}{L_z(0)}}{U(a,b,c)} \qquad (3.15\ (d))$$

In [47] the voltage V is defined as the averaged potential difference between the "top" and the "bottom" of the particle. I_{pol} the displacement current is defined as the integral flux of the displacement current flowing across the top or bottom terminal of the nanoparticle, $\mathbf{J_d} = -i\omega \boldsymbol{D}$, where $\boldsymbol{D}$ is the local electric displacement vector, that satisfies Kirchhoff's current and voltage laws. In this way these definitions describe a physical analogy and complete correspondence between the scattering problem of an isolated ellipsoidal particle (figure 6 (a)) and its equivalent circuit representation in terms of its impedance Z_{nano} (figure 6 (b)). The external exciting field can be related with I_{imp} that is the amplitude of an impressed current generator and the dipolar fields around the nanoparticles associated with a parallel fringe capacitance of impedance Z_{fringe} .[47]

Varying the aspect ratio of the ellipsoid or the orientation of the exciting electric field we can modify the effective impedance associated with the nanoparticle, it can add effectively new degrees of freedom to the possibility of synthesizing the desired circuit response with an isolated dielectric or plasmonic nanoparticle. The impedance Z_{nano} enters into resonance with Z_{fringe} in the circuit of figure 6 when $Z_{fringe} = -Z_{nano}$ i.e., for

$$\varepsilon = \frac{1 - L_z(0)}{L_z(0)} \varepsilon_0 \qquad (3.16)$$

3.5 Coated ellipsoid, equivalent circuit and field enhancement

Based on the discussions in pervious sections in this chapter, we can consider a coated ellipsoid and develop its equivalent circuit model. Silver, gold and aluminum as metal nanoparticles and silicon dioxide(SiO_2), glass and aluminium oxide(Al_2O_3) as coating materials, can be used to study the behavior of coated ellipsoid, as shown in figure 7. Metal

nanoparticles and nanoshells consisting of metal shells and dielectric cores are known to enhance incident electromagnetic fields around themselves due to surface plasmons. The field enhancement factors can be calculated for spherical metal nanoparticles and nanoshells in the quasistatic limit using empirical wavelength-dependent dielectric constants.

Figure 7 - Metallic ellipsoid coated with dielectric.

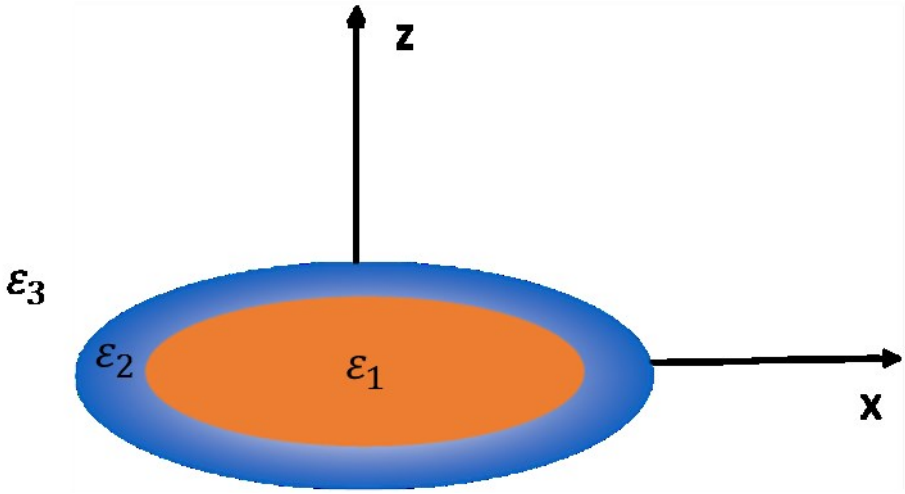

Source: The Author, 2019.

We will investigate the dependence of the field enhancement factor on various parameters such as metal element, wavelength, surrounding medium, dielectric core material and diameter ratio between the core and the shell. By adjusting the relative core and shell dimensions, we can widely tune the resonance frequency, or the peak wavelength for field enhancement, of a nanoellipsoid, while the optical resonance is essentially a fixed frequency resonance, almost independent of their particle sizes for metal nanospheres. Also, nanoellipsoid can exhibit significantly larger field enhancement than that for nanoparticles according to conditions. We will apply the quasistatic analysis to find the intensities of electromagnetic fields around subwavelength-size metal nanoparticles and nanoellipsoid.

3.6 Nanosphere

In this section we discuss the materials required for the preparation of silver and gold nanospheres and the synthesis of silver and gold nanospheres. The characterization of nanoparticles is explained in 3.6.3 in details.

3.6.1 Materials

Silver nitrate ($AgNO_3$, 99.9999%) was purchased from Aldrich. The reactions were carried out using Sodium borohydrate (Sigma Aldrich), Trissodium citrate (TSC) (Sigma Aldrich), ascorbic acid (Neon chemistry) and sodium poly 4-styrene sulfonate (PSSS), that was purchased from Sigma Aldrich. For gold nanoparticles, $HAuCl_4$ was purchased from (Sigma Aldrich) as well.

3.6.2 Synthesis of silver nanospheres

To prepare spherical silver nanoparticles, silver nitrate and trisodium citrate were used as starting materials, using the methodology adapted by Lee and Meisel (1982), based on chemical reduction. [96] In an Erlenmeyer flask, 25 ml of 0.001 M $AgNO_3$ was heated to boil using magnetic stirring (800 rpm), followed by the addition of 5 ml of trisodium citrate (TSC) 1% drop by drop until the change of color until pale yellow. The solution was kept stirring until the change of the solution to gold yellow and was stored for further characterization. The mechanism of reaction could be expressed as follows:

$$4Ag^{+} + C_6H_5O_7Na_3 + 2H_2O \rightarrow 4Ag^{o} + C_6H_5O_7NaH_3 + 3Na^{+} + H^{+} + O_2 \uparrow \quad (3.17)$$

3.6.3 Synthesis of gold nanospheres

The chemicals required for this procedure are Hydrogen tetrachloroaurate ($HAuCl_4$) and trisodium citrate. Au^{+3} ions are reduced to neutral gold atoms, where citrate ions act as both reducing agent and capping agent. In an Erlenmeyer, 20 ml of 0.001M HAuCl4 was added, and 5 ml of a 1% solution of TSC was quickly added to the rapidly-stirred (800 rpm) boiling solution. The gold solution gradually forms as the citrate reduces the Au^{+3}. The solution was removed from heating when the solution has turned deep red or 10 minutes has elapsed. As a result of this process gold nanoparticles were synthesized and were confirmed by the color change since the gold nanoparticles are red in color. To synthesize gold nanoparticles again citrate reduction method was used. The reason for choosing this method is that the citrate method can produce quality particles up to ~50 nm in size, beyond which the particles are non-spherical. [28]

3.6. 4 Colloidal NPs characterization

Ag and Au NPs were characterized using UV-Vis, and SEM. The spectra was recorded on Thermo Scientific Evolution 600S spectrofotometer, with a scanning range from 350 nm to 720 nm and 450 nm to 720 nm in the case of silver and gold, respectively. A base line was set using ultrapure water.

Figure 8 – characterization of silver and gold nanosphere.

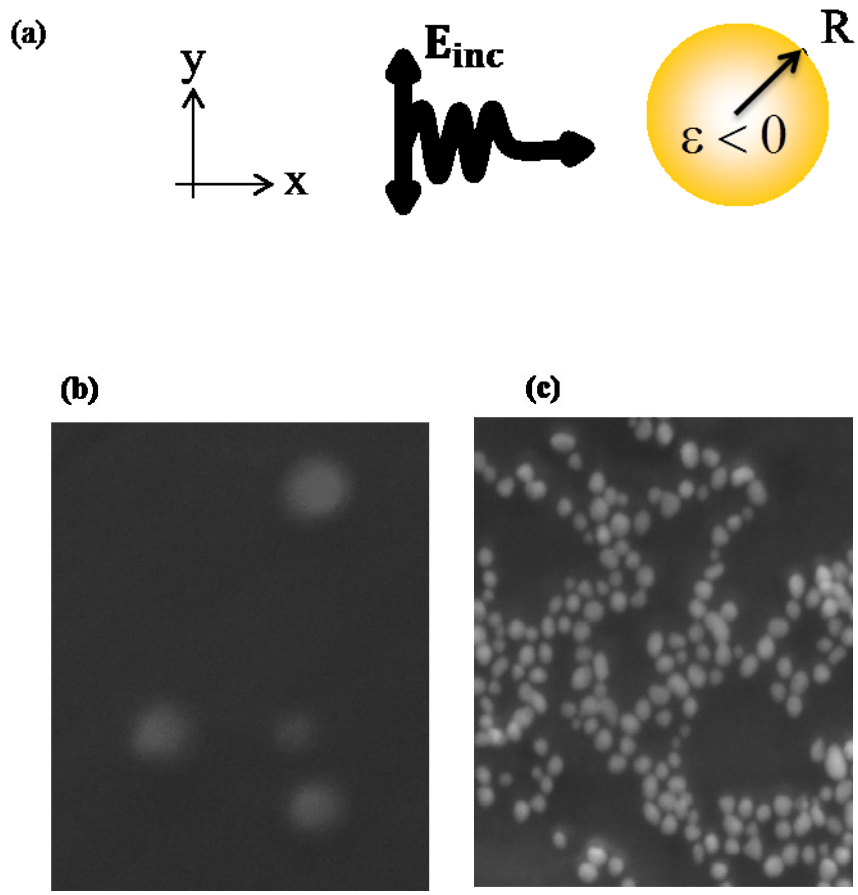

Source: The Author, 2019.

Note: (a) Plane wave incident on silver/gold nanosphere, (b) scanning electron microscopy (SEM) image of silver, (c) gold nanosphere.

The synthesis was determined by observation of a plasmon resonance band and their $\lambda_{máx}$ value. Data plot was designed using Origin Pro. The analysis was obtained using Zetasizer ZS90 (Marlven, UK). Briefly, the samples were diluted and inserted into a specific acrylic cuvette (DTS 0012 or DTS1060 microelectrophoretic cell). All the measurements were made in triplicate. A few drops of colloidal solution were allowed to dry on an aluminum paper, on

ambiental temperature. Later, SEM microscopy was performed using MIRA 3 TESCAN operated at 20 kV. Data was analyzed using ImageJ software. Silver nanospheres of radius R = 23 ± 2 nm and gold nanospheres of radius R = 10 ± 1.6 nm in water suspension were prepared in lab as shown in figure 8(b) and figure 8(c).

3.7 Nanoprism

This section is divided into three subsections: materials required for the nanoprisms, sysnthesis of spherical silver nanoparticles and Synthesis of silver nanoprisms using the seed-mediated method. The details of each section are given below.

3.7.1 Materials

Silver nitrate ($AgNO_3$, 99.9999%) was purchased from Aldrich. The reaction were carried out using Sodium borohydrate (Sigma Aldrich), Trissodium citrate (TSC. Sigma Aldrich), Ascorbic acid (Neon chemistry) and Sodium poly 4-styrene sulfonate (PSSS), that was purchased from Sigma Aldrich.

3.7.2 Synthesis of spherical AgNPs

To prepare spherical silver nanoparticles, silver nitrate and trisodium citrate were used as starting materials, using the methodology adapted by Lee and Meisel [96], based on chemical reduction. In an Erlenmeyer flask, 25 ml of 0.001 M $AgNO_3$ was heated to boil using magnetic stirring (800 rpm), followed by the addition of 5 ml of trisodium citrate (TSC) 1% drop by drop until the change of color until pale yellow. The solution was kept stirring until the change of the solution to gold yellow and was stored for further characterization. The mechanism of reaction could be expressed same as shown in equation (3.17) and we rewrite here

$$4Ag^{+} + C_6H_5O_7Na_3 + 2H_2O \rightarrow 4Ag^{o} + C_6H_5O_7NaH_3 + 3Na^{+} + H^{+} + O_2 \uparrow$$

3.7.3 Synthesis of silver nanoprisms using the seed-mediated method

The methodology was adapted following the work of Aherne et. al. [97] In a typical experiment, silver seeds were produced in an aqueous medium by combining TSC (5 ml, 2.5 $mmol.l^{-1}$), solution of the desired polymer PSSS, PVA, $NaPO_3$ and CBP (0.25 ml, 500 $mg.l^{-1}$)

and $NaBH_4$ (0.3 ml, 10 mmol. l^{-1}, freshly prepared), followed by the addition of aqueous $AgNO_3$ solution (5 ml, 0.5 mmol.l^{-1}, dropwise) .The growth was prepared using 5 ml of deionized water, ascorbic acid (75 µl, 10 mmol.l^{-1}) and different amounts of seed colloids (90, 200, 500, and 650 µl) followed by the addition of more $AgNO_3$ solution (3 ml, 0.5 mmol. l^{-1}). All the colloids was kept on refrigeration until further characterization.

3.8 Colloidal NPs characterization

Ag nanoprisms were characterized using Uv-Vis, and SEM. The spectra was recorded on Thermo Scientific Evolution 600S spectrofotometer, with a scanning range from *350 nm* to *720 nm*. A base line was set using ultrapure water. The synthesis was determined by observation of a plasmon resonance band and their $\lambda_{máx}$ value. Data plot was designed using Origin Pro. The analysis was obtained using Zetasizer ZS90 (Marlven, UK). Briefly, the samples were diluted and inserted into a specific acrylic cuvette (DTS 0012 or DTS1060 microelectrophoretic cell). All the measurements were made in triplicate. A few drops of colloidal solution were allowed to dry on an aluminum paper, in ambiental temperature. Later, SEM microscopy was performed using MIRA 3 TESCAN operated at 20 kV. Data was analyzed using ImageJ software.

3.9 Numerical Analysis

The numerical modeling of nanoslits, nanospheres, nanoellipsoids and nanoprisms was performed using finite element method (FEM) with COMSOL Multiphysics. Proper boundary conditions were applied in all cases of nanoslit to avoid the reflections. Spherical perfectly-matched-layer, 10 times greater than the radius of nano sphere was used to enclose the simulation volume and to avoid unnecessary reflections for the cases of nanospheres, nanoellipsoids and nanoprisms further proper boundary conditions were applied to study the optical properties of these nanoprticles. Optical data from Johnson and Christy [(22)] was used to model the dielectric functions of the both materials, i.e., silver and gold. The magnitude of the background electric field was set 1 V/m for all cases for all types of nanoparticles.

Figure 9 - Tertrahidral meshing of spherical object.

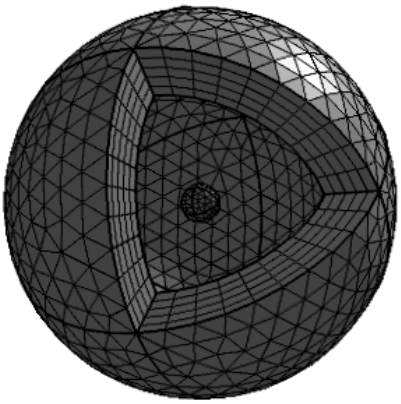

Source: The Author, 2019.

To justify the validity of our results obtained during the simulations here we demonstrate two examples where we reproduced the results from published literature. [91-92] In our first example we consider a nanoslit composed of silver as assumed in. [91] The adopted values for the slit from [91] include the thickness of the slit t = 700 nm and width of W= 100 nm.

Figure 10 – Electromagnetic properties of nanosphere.

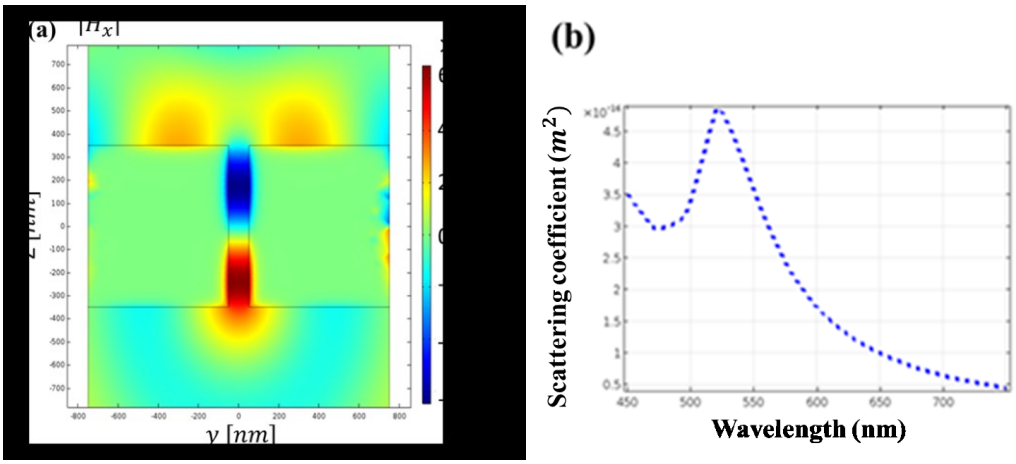

Source: The Author, 2019.

Note: (a) Magnetic field component of nanoslit composed of silver [91], (b) scattering coefficient of nano gold sphere [92].

Using these parameters we plotted magnetic field component H_x of magnetic field as shown in figure 10 (a). In second example, we consider a single gold nanosphere with radius a = 30 nm

[92] excited by a uniform electric field, its corresponding scattering measurement is reported in figure 10(b), showing a clear resonant peak around 530 nm.

These two examples demonstrated in figure 10 show excellent correspondence with the results published in literature. [91-92] Based on these examples we can conclude that our numerical simulations are in correct order. On the bases of these materials and methods we discussed in this chapter we will present our results in next chapter.

4 RESULTS AND DISCUSSIONS

In this chapter we will discuss the results based on the materials and methods discussed in chapter 3. We will explain the optical properties of nanoslit, nanosphere, nanoellipsoid and nanoprism in this chapter. Further we explain how we can design equivalent nanocircuit for nanosphere based on optical properties of nanosphere.

4.1 Optical properties of nanoslit

Plasma frequency in certain metals such as silver and gold, is in the ultraviolet or visible regimes, at the optical frequencies these metals behave as plasmonic materials, i.e., the real part of their permittivity is negative. [14] As a result, the interaction between optical signals and plasmonic nanoparticles involves surface plasmon resonances. [15]

Numerical simulations are performed using finite element method (FEM) with COMSOL multiphysics. The metals, silver and gold, are used and their dielectric functions are modeled using optical data from Johnson and Christy. [22] The results are expressed in terms of electric field, magnetic field and the power flow for transverse magnetic or *p*-polarization.

In the following discussion we explain how field enhancement occurs. In figure 11(a) a very small amount of electric field is present at metal-dielectric interface, this amount of electric field is enough to sustain the surface current $\boldsymbol{J}$ and this current $\boldsymbol{J}$ sustains the magnetic field above the surface as shown in figure 11 (b) and justifies the continuity conditions of electric and magnetic field across the interface.

Figure 11 (b) shows the corresponding magnetic field. The reflected electric and magnetic fields interfere with the incident electric and magnetic fields and as a result they produce a standing wave above the interface. At the sharp edges of the slit, there exists electric dipole because the current $\boldsymbol{J}$ stops at the edges of the slit and allow the accumulation of charges at the sharp corners and these oscillating charges on the opposite edges of the slit behave as an electric dipole. These electric dipoles can be observed at the top and bottom of figure 11 (a). It is considered that these dipoles contribute in the field enhancement alongside the surface plasmons on the metal-dielectric-metal interface. [11] Inside the waveguide the surface charges and currents, carry the traveling beam downward. When this traveling beam reaches at the bottom of the waveguide it encounters an impedance mismatching and at this end accumulation of charges give rise a second electric dipole as it can be viewed in figure 11 (a),

this strong dipole generates an upward-traveling wave inside the waveguide. The opposite travelling beams generate a standing wave inside the waveguide.

Figure 11 - Gold-gold slit of width $w = 50\ nm$ in a metallic structure of thickness $t = 500\ nm$.

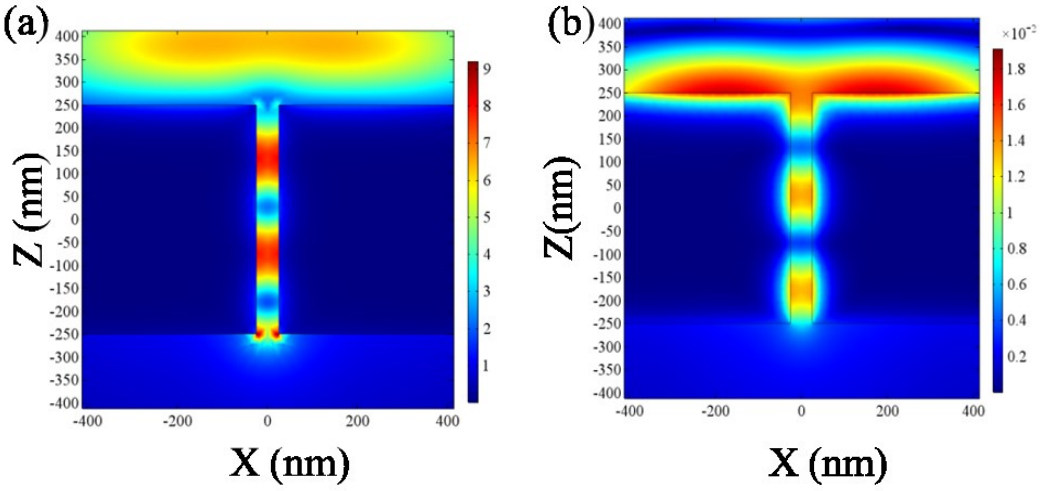

Source: The Author, 2019.

Note: (a) Electric field distribution, (b) magnetic field, under *p*-wave illumination at the wavelength λ = 633 *nm*.

Top of figure 11 (a) outside of the slit present's total field as the sum of incident, scattered and reflected field. We observe a maximum value of enhanced field up to 9 times in figure 11 (a). These results show that the pattern of the *E*-field amplitude at the beginning of the slit at the top surface clearly reveals the localized character of the resonance and its dipolar nature. The figure 11 (a) also show that the *E*-field intensity maxima are at the edges of the slit.

As we are going to deal with different materials so for the sake of comparison using the same parameters used in figure 11, we further investigate field enhancement and amount of power present inside the waveguide. For this purpose, first we considered the slit composed of silver slabs separated by the width of the slit 50 *nm* and we assumed the waveguide length 500 *nm* as shown in figure 12.

In figure 12 (a) only one strong dipole exits at the bottom of the slit and the amount of the charges at the top edges of the slit is reduced. Field enhancement in this case is 6 times of the incident field. By comparing this result with figure 11(a) the electric field enhancement is reduced up to 3 times.

Figure 12 - Silver-silver slit of width $w = 50\ nm$ in a metallic structure of thickness $t = 500\ nm$.

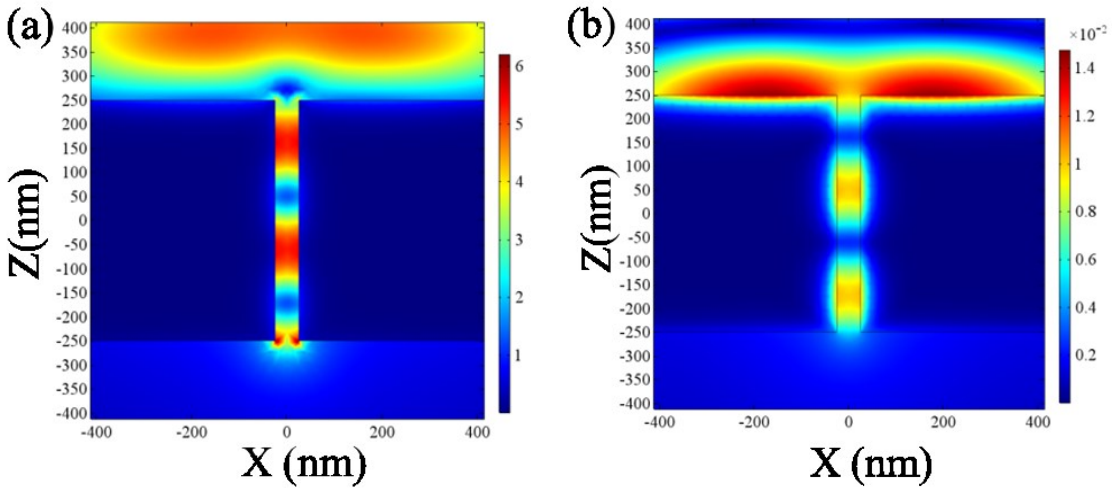

Source: The Author, 2019.

Note: (a) electric field distribution (b) magnetic field, under *p*-wave illumination at the wavelength $\lambda = 633\ nm$.

Here we demonstrate an example how we can tailor the value of enhanced electric field and power flow. We considered a slit composed of silver and gold and observed the interesting results as shown in figure 13. Figure 13(a) presenting the electric field, as we observed in figure 11(a) and figure 12(a), the value of enhanced electric field is 2 times less as compare to gold nano slit and 1 time higher as compare to silver nano slit suggesting that this configuration is helpful to adjust the value of electric field. Similarly the analysis of figure 11(b), 12(b) and 13(b) indicates that values obtained for magnetic field in figure 13 (b) are less than figure 11(b) and higher as compare to figure 12(b), respectively. By using this configuration the values obtained for electric field and magnetic field are in-between the values obtained for electic field and magnetic field using gold slit in figure 11 and silver slit in figure 12. It proves that by using different combinations of materials we can adjust the values of electromagnetic fields and power flow as per required.

The desired response of the system can be obtained by modeling the parameters including refractive index of surrounding medium, permittivity and permeability of the materials used for the slit and by adjusting the subwavelength parameters of the nano slit. On the basis of the results shown from figure 11 to figure 13 it is observed that, the reflection and transmission inside the slab generates the Fabry–Perot resonance at the entrance and the exit of the slab when we observe the behavior of electric field.

Figure 13 - Silver-gold slit of width *w = 50 nm* in a metallic structure of thickness *t = 500 nm.*

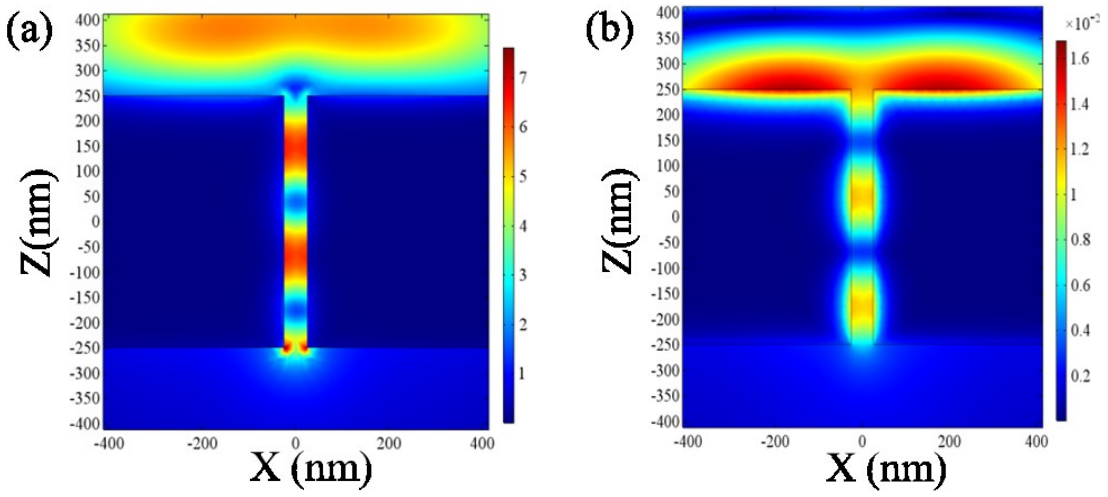

Source: The Author, 2019.

Note: (a) electric field (E_x) distribution (colors in *V/m* units) (b) magnetic field (H_y) (in *A/m* units), under *p*-wave illumination at the wavelength $\lambda = 633$ *nm*.

The nanoslit in the plasmonic slab, regardless of how narrow that is, for TM mode always supports a propagating state. Even though we considered just a single wavelength but these models can be used for broader range of frequencies.

The interface between metal and dielectric medium has major significance; one may consider different dielectric material else then free space and can study the behavior.

4.2 Power flow in nanoslit

When plane wave propagating from top (air) reaches at the air-metal interface as we considered the situation in figure 11, most part of power is reflected back to air and only a small part of incident power is transmitted to the metal as the skin depth is only a few nanometers so the energy flux or the power flow penetrates only a few tens of nanometers. The power penetrating into the metal is given by [12]

$$\mathrm{P} = \frac{1}{2} Re[\mathrm{S}] = \frac{|E_0|^2}{Z_0} . \frac{2k_0\delta}{2 + 2k_0\delta + (k_0\delta)^2} \qquad (4.1)$$

At air-metal (silver or gold) interface, the cycle-averaged incident power is

$$P_i = \frac{|E_0|^2}{2Z_0} \qquad (4.2)$$

Figure 14 – Power Flow in nanoslit

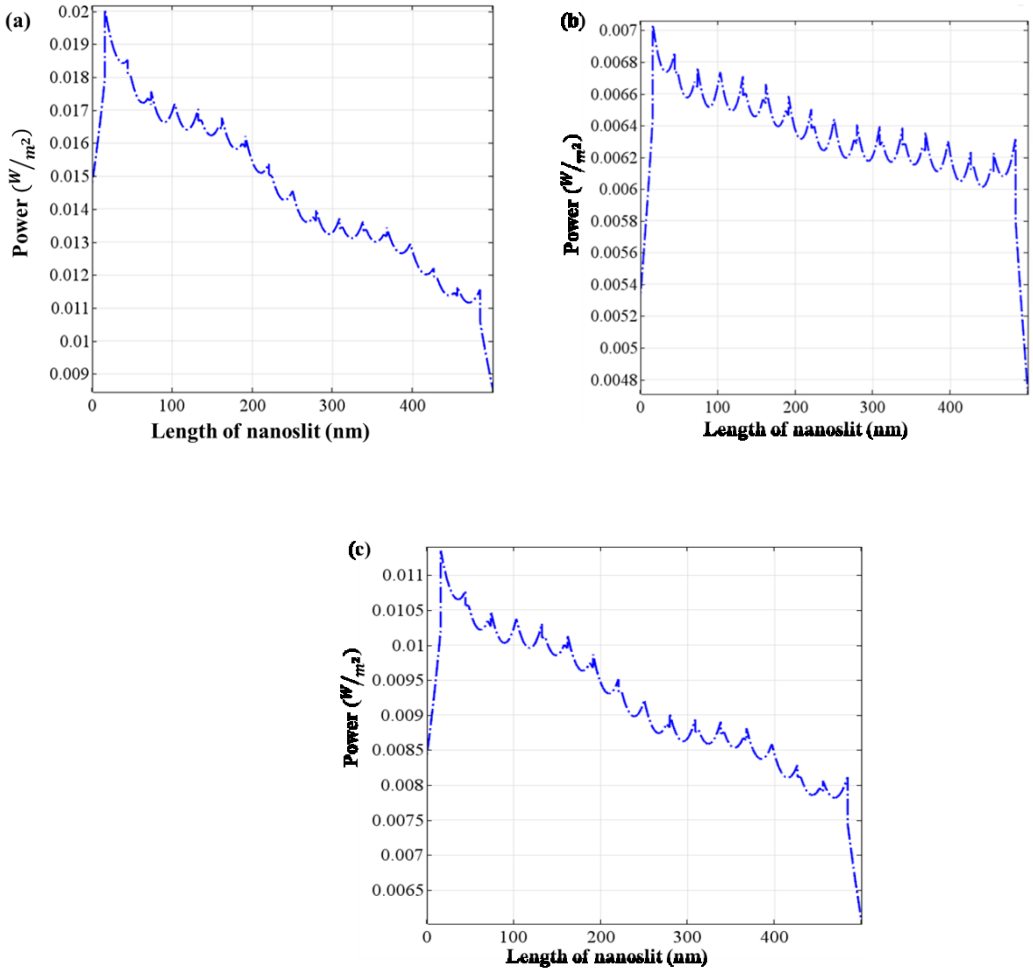

Source: The Author, 2019.

Note: (a) gold nanoslit (b) silver nanoslit (c) silver-gold nanoslit, Power flow (in W/m^2 units) under *p*-wave illumination at the wavelength λ = 633 *nm* inside of nanoslit of width *w = 50 nm* and thickness *t = 500 nm*.

And therefore the fraction of the incident power entering the metal is:

$$\frac{P}{P_i} = 2k_0\delta \qquad (4.3)$$

The reflected power is given by

$$P_r = -|R|^2 \frac{|E_0|^2}{2Z_0} \qquad (4.4)$$

And the fraction of the incident power reflected is

$$\frac{P_r}{P_i} \approx (1 - 2k_0\delta) \qquad (4.5)$$

Figure 14 (a) presents the power flow inside the waveguide. Fabry–Perot resonances occur inside the waveguide and metal (gold) losses decrease the power flow inside the waveguide. The width of the slit effects Fabry Perot resonances. From figure 14 (a)-(c), it is observed for all cases that the power flow inside the slit decreases as long as the length of waveguide increases. This loss in power flow mainly occurs because of internal losses of metals considered for different cases. Inside the waveguide, for the case of gold nanoslit as shown in figure 14 (a) the power decreases from its maximum value 2×10^{-2} to 1.1×10^{-2} . For the case of silver nanoslit (figure 14 (b)) the power decreases to 0.7×10^{-2} from 0.63×10^{-2}. Finally, for the case of silver-gold nanoslit (figure 14 (c)) the power decreases from 1.1×10^{-2} to 0.8×10^{-2}. In all these three cases the length of waveguide is 500 *nm.* The power flow scheme also justify our consideration that if we use silver-gold nanoslit we can obtain intermediate value of enhanced electric field and power going outside of the nanoslit.

4.3 Electric field enhancement and power transmission in nanoslit using nanocavity

In different cases we assumed from figures (11-13) we observed that in every case we observed enhanced value of electric field. If we want to transfer power from one end to other end of the slit, amount of power transfer is low and the reason behind this phenomenon is impedance mismatching at the boundary of metal-dielectric interface. So in this section, we particularly focus on power flow inside the slit and possibility of field enhancement. We will discuss three different models that can be used to enhance both electric field and power. These models are modified by keeping in mind the concept of impedance matching so that we can reduce the power reflection.

In this section we will show numerically that a compact structure, consisting of different types of nanocavities at the entrance of a subwavelength plasmonic slit, can lead to enhanced transmission through slit. These nanocavities can increase resonant transmission enhancement. In addition the nanocavities can improve the impedance matching. An optimized structure at the entrance of the slit can lead larger transmission cross section compared to the optimized reference slit without nanocavities. Using single microcavity at the entrance and exit of a subwavelength plasmonic slit, the transmission cross section of the slit can be enhanced. [17, 18] Use of multiple microcavities can be used to enhance the coupling efficiency of slit [19] on the other hand it was demonstrated that using multiple microcavities at the entrance and exit sides of a subwavelength slit and filling with absorbing material can be used to enhance the absorption cross section of the slit as well. [20]

The use of nanocavities can enhance the incoupling of normally incident light from free space into the slit mode and the outcoming of light from the slit mode to free space radiation in the normal direction. In this work consider nanocavity where we are using single wavelength but these models can be studied using broad range of frequencies. Here we consider a nanoslit composed of gold, silver or silver-gold structure with X nanocavities at the entrance. All the considered structures are compact will all nanocavities dimensions limited to less than operating wavelength 633 nm. We use finite element method (FEM) using COMSOL Multiphysics to calculate the power transmission through the structure and the field enhancement. Using this method we can use the experimental data for the frequency dependent dielectric constant of metal such as gold and silver [22] to model the optical properties. Perfectly matched layer absorbing boundary conditions at all boundaries of the simulation domain are also used. [21]

In first step, we analyze a structure with a single nanocavity (X) at the entrance of the slit as shown in figure 15 with X = 1. Using this structure we want to study the effect on field enhancement and power flow. This structure is optimized at a single wavelength 633 nm however this structure can be used to operate at other wavelengths at near-infrared and visible. All the nanocavity dimensions are limited to less than 633 nm and we are addressing asymmetric structure. Thus, for the optimized (X=1) structure the presence of the nanocavity at the entrance results in significantly larger field enhancement and much higher values of power for all cases considered in figure 15.

In all cases, our reference structure is nanoslit composed of that material without nanocavity, first we discuss the structure composed of gold. As shown in figure 15(a) electric field enhancement is 1.56 times higher as compare to electric field enhancement in figure 11(a). On the other hand the amount of power flow is 2.8 times higher in figure 15 (b) as compare to figure 14(a). So these results in figure 15 indicating that using nanocavity it is possible to achieve higher values of electric field and power transmission. In the case of silver as shown in figure 15 (c) field enhancement is 2 times higher as compare to figure 12 (a) and power flow in figure 15 (d) is 4.29 time higher as compare to figure 14(b). Finally, for the case of silver-gold structure the field enhancement is 2.28 times higher in figure 15(d) as compare to figure 13 (a) and amount of power is 4.55 times increased in figure 15(e) as compare to figure 14(c).

This structure can be considered as a system of two coupled resonators, the silt and the nanocavity at the entrance of the slit. These are also coupled to free space propagating plane waves above the structure as well as to plasmonic modes at the top of metal surface.

The nanocavity can be considered as a plasmonic transmission line which is short circuited on one side and open-circuited on the other. [22] To consider the Fabry-Perot resonance condition for nanocavities, the first resonant length of the microcavity is $\frac{\lambda_0}{4}$ which for $\lambda_0 = 633nm$ gives 158.25 nm.

To study the effect of nanocavity on electric field enhancement and power flow here we consider multiple nanocavities at the entrance of the slit (figure 16). More specifically, we use (X = 2) in such a way that the widths and lengths of nanocaivties are less then $\lambda_0 = 633nm$. In this case, the nanocavities at the entrance of the slit greatly enhance the coupling between the free space waves and the slit mode. This is consistent with previous studies that optimized multi section structures can be used to improve the impedance matching and therefore the coupling between optical modes. [19, 23] In the case of optimized single nanocavity structure where the increased transmission is associated with increased resonance enhancement in the slit, for optimized double nanocavity structure the increased transmission is mostly associated with improved impedance matching between free space waves and the slit modes. For gold nanoslit with double nanocavities at the entrance, field enhancement is 1.78 times higher and power flow is 2.8 times higher as compare to gold slit without nanocavity at the entrance as shown in figure 16 (a-b).

Whereas, for silver nanostructure we observer 2.33 times increase in electric field (figure 16(c)) with respect to our reference slit in figure 12 (a) and 4.29 times higher amount of power is recorded (figure 16 (d)) as compare to figure 14 (b). Finally, for silver-gold slit with double nanocavity at the entrance we found 2.57 times higher electric field (figure 16 (e)) as compare to shown in figure 13 (a) and 4.55 times higher value of power (figure 16 (f)) as compare to figure 14 (c). In both cases we assumed so far for nanocavities showed excellent way to improve the electric field enhancement and amount of power flow as well. Still we observe that even these structures offering excellent electric filed enhancement and better amount of power flow from the system, there are some accumulation of charges at the edges of nanocavities, which may cause reflections and can reduce the required outcomes. To minimize the reflection and increase the value of electric field enhancement and power flow, here we introduce new type of nanocavity as shown in figure 17. Our results show that this

type of nanocavity is useful to increase the impedance matching and can be used to minimize the reflections from the interface. We deign this geometry in such a way that it does not contain the edges at its interfaces. This circular cavity at the entrance of nanoslit provides higher values as compare to the results of reference nanoslits shown in figures (11-16).

In figure 17 (a) for gold nanostructure, we notice 1.33 times higher value of enhanced electric field. The amount of power is 2 times higher as compare to our reference slit in figure 13 (a). Whereas, for silver nanostructure we observer 1.33 times increase in electric field (figure 17 (c)) with respect to our reference slit in figure 12 (a) and 2.57 times higher amount of power is recorded (figure 17 (d)) as compare to figure 14 (b). Finally, for power (figure 17 (f)) as compare to figure 14 (c) is calculated. In this section we have demonstrated successfully that how one can improve the amount of electric field and power flow inside of the nanoslit with nanocavity at its entrance for different combinations of these metals. This introduction of nanocavity can be presented in equivalent circuit by introducing a parallel impedance to impedance (Z_1) in figure 2 (b). It may be useful to include the nanocavity at the exit of nanostructures presented in figures (15-17) to obtain required results as explained in [23] for microcavities. By applying such nanocavities corresponding components will be required to model equivalent circuit. In this work, as we focused on designing new type of proposed nano structure composed of silver-gold combination, that can be used to obtain the intermediate values that are less than the values obtained on the case of gold and higher as compare to silver structures.

Figure 15 - Nanoslit with nanocavity at the entrance of width *w1 = 150 nm* and thickness *t1 = 50 nm* while the width of nanoslit *w = 50 nm and* thickness *t = 450 nm*.

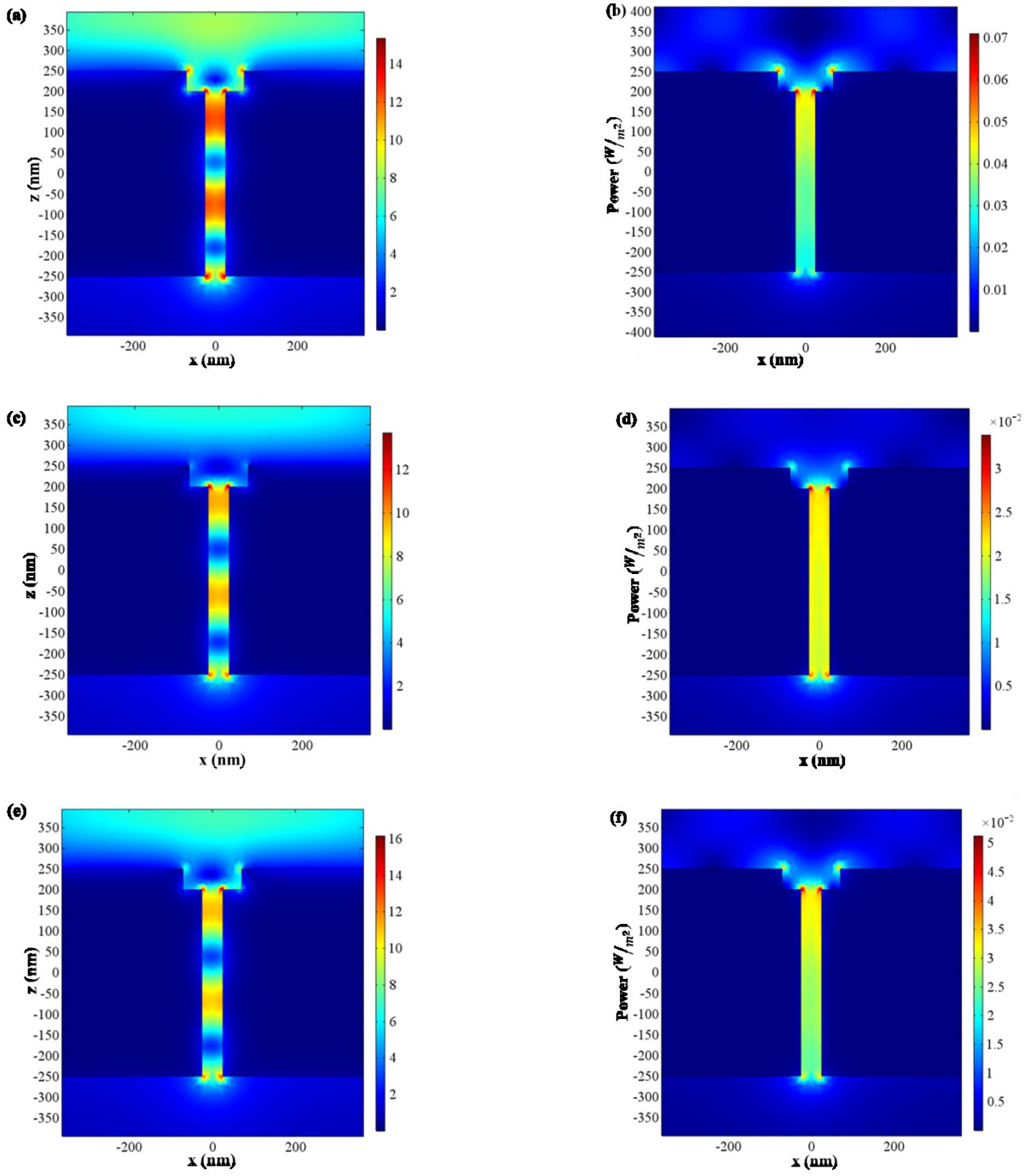

Source: The Author, 2019.

Note: (a), (c) and (e) electric field distribution (colors in *V/m* units) and corresponding power flow (in W / m^2 units) in (b), (d) and (f) for gold-gold, silver-silver and silver-gold structures, respectively, under *p*-wave illumination at the wavelength $\lambda = 633$ *nm*.

Figure 16 - Nanoslit with nanocavity at the entrance of width *w1 = 150 nm* and thickness *t1 = 25 nm* and width *w = 130 nm* and thickness *t2 = 25 nm* while the width of nanoslit *w = 50 nm and* thickness *t = 450 nm*.

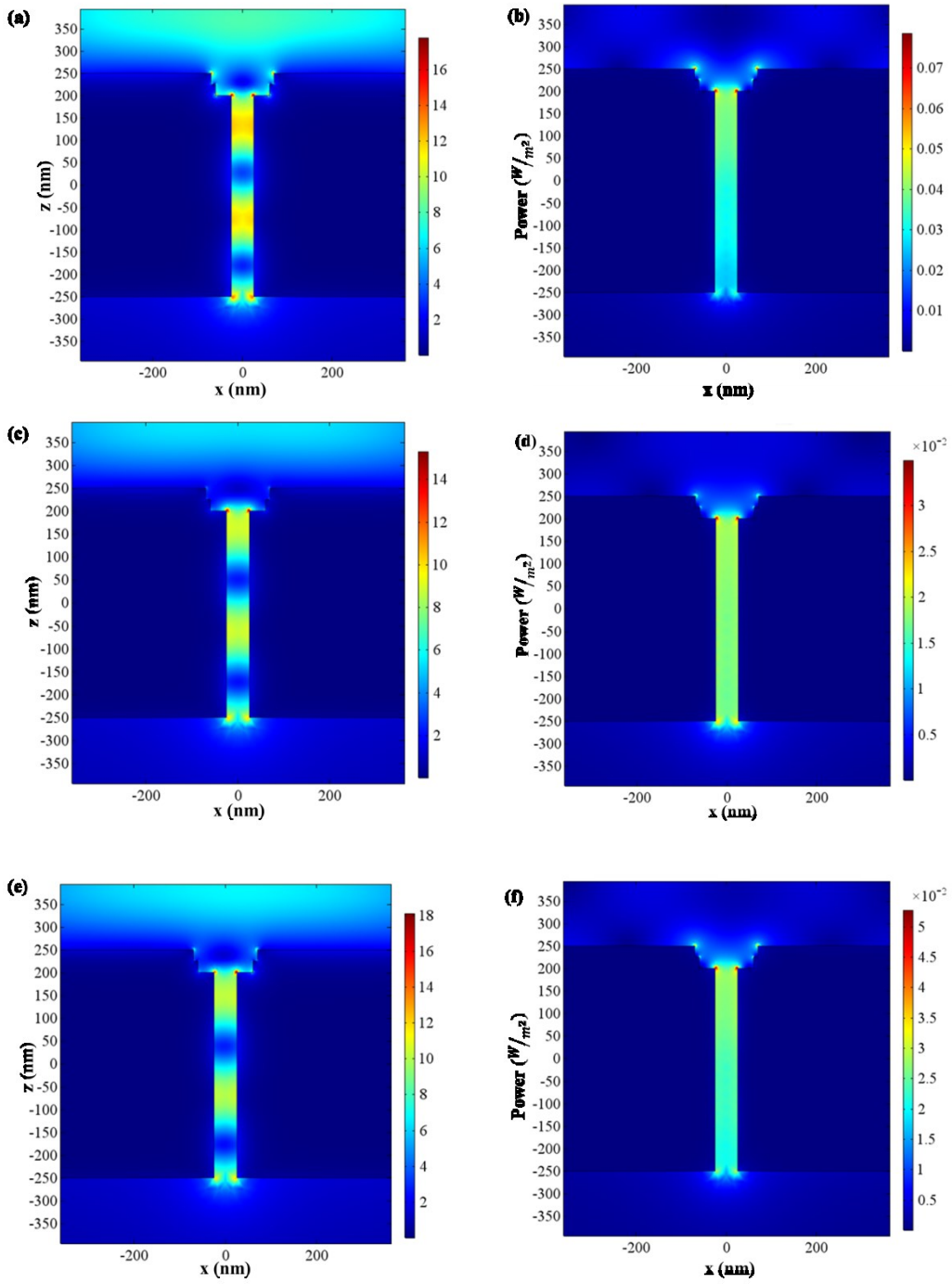

Source: The Author, 2019.

Note: (a), (c) and (e) electric field distribution (colors in *V/m* units) and corresponding power flow (in W/m^2 units) in (b), (d) and (f) for gold-gold, silver-silver and silver-gold structures respectively, under *p*-wave illumination at the wavelength $\lambda = 633$ *nm*.

Figure 17 - Nanoslit with nanocavity at the entrance of width *w1 = 280 nm* and thickness *t1 = 140 nm* while the width of nanoslit *w = 50 nm and* thickness *t = 360 nm*.

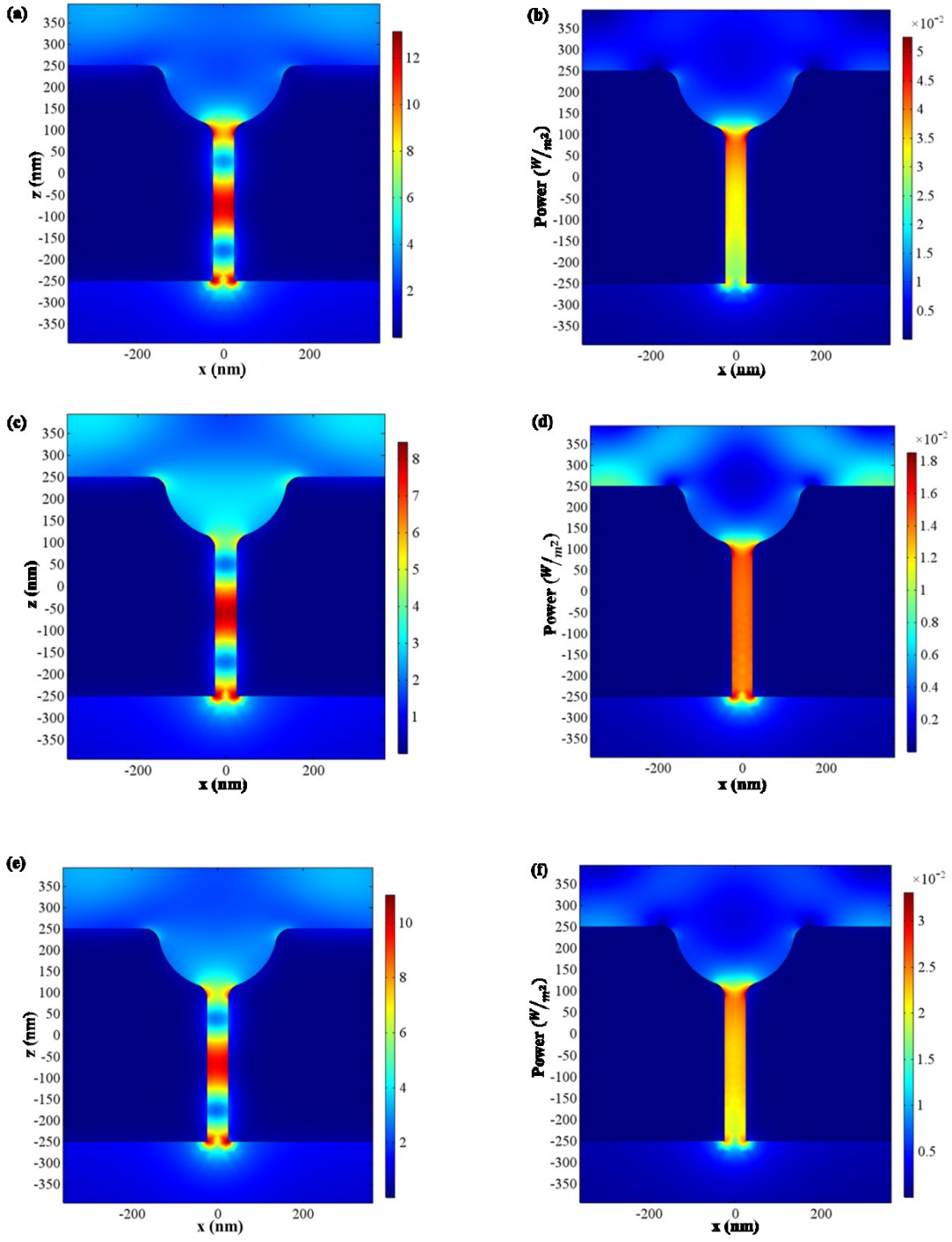

Source: The Author, 2019.

Note: (a), (c) and (e) electric field distribution (colors in *V/m* units) and corresponding power flow (in W/m^2 units) in (b), (d) and (f) for gold-gold, silver-silver and silver-gold structures, respectively, under *p*-wave illumination at the wavelength $\lambda = 633$ *nm*.

In future, these interesting results will courage the researchers to apply different combinations of materials. This concept of nanoslit is like a device that can be used to control the required outputs. One may just change the material inside the slit instead of free space that we considered here and can study new problem or even it is possible to use different materials to design the nanoslit. The other controlling possibilities are the parameters of nanoslit. As we studied (not shown in this work) that the height and width of nanoslit plays key role to enhance the parameters of incident light so one may use this option such that fulfilling the subwavelength requirement to design the parameters of slit.

4.4 Numerical analysis for nanosphere

For many applications in nanoplasmonics, silver and gold are used widely. Silver has intense plasmonic response while gold is known for its easier functionalization and localized plasmon resonances in the visible infrared range. [29] Here we discuss the optical properties of both materials in details.

In figure 18, electric field $|E/E_0|$ is shown for gold and silver sphere at resonance wavelengths. At the interface between water and silver or gold, due to higher conductivities of silver and gold nanoparticles, show higher values of the field enhancement. In figure 18(a), the enhanced value of electric field is ~6 times while for silver sphere figure 18(b) of same radius (r = 10 nm) electric field enhancement at the interface is 3.29 times higher as compare to incident electric field. The maximum values observed in these results are associated with the resonances or surface mode. Usually the peak value of the field enhancement factor is around the wavelength where

$$\varepsilon_1 = -2\varepsilon_2$$

Where ε_1 and ε_2 are the permittivities of the sphere and the surrounding medium, respectively. For all wavelengths considered for both silver and gold nanospheres, we observed that the electric field map shows the typical two-lobe distribution corresponding to an electric dipole oriented along the *x* axis of different amplitudes depending on the type of the material and corresponding wavelength. Whereas in the case of silver nanosphere (around r = 50 nm) Albeit, four lobs are possible presenting quadropole mode distribution.

Extinction cross section of small nanoparticles is the sum of scattering cross section and absorption cross section of nanoparticles. Enhanced electric field expresses the ability of the nanosphere to increase the electric field at its vicinity that is dominant parameter for various

applications including surface-enhanced Raman spectroscopy (SERS) or molecule sensing. On the other hand, electric field inside the sphere is directly related to the ability of nanosphere to generate heat so the Joule effect is directly linked to the magnitude of the electric field inside the nanosphere.

Figure 18 - Enhancement of electric field (in V/m units) at plasmonic resonances.

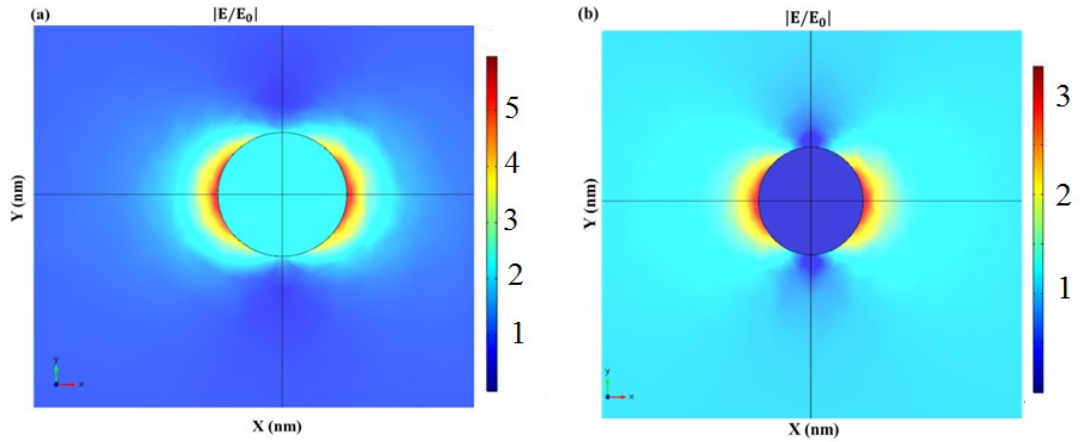

Source: The Author, 2019.

Note: (a) λ = 530 nm for gold nanosphere, (b) λ = 355 nm of silver nanosphere (radius r =10 nm) under p-wave illumination.

In figure 19, the extinction cross section of silver and gold nanoparticles is presented. For silver and gold sphere resonance peak for sphere of radius (r = 10, 15, 20, 25, 30, 35, 40, 45 and 50 nm) are considered. For both silver and gold sphere red shift in the wavelength is observed as the radius of sphere gets larger. For gold sphere, the resonance peak for sphere (r =10 nm) is at 525 nm and as the size of sphere increases this resonance peak moves towards higher values of wavelength, i.e., for (r = 50 nm) the resonance peak is at 550 nm. For silver sphere the resonance peak for (r=10 nm) is at 354 nm and with increase in size of sphere the red shifted resonance peak is observed as shown in figure 19 (b), for example, for silver sphere (r = 50 nm) the resonance peak is at 394 nm. The contribution of scattering and absorption cross section to extinction cross section changes depending on the size of nanoparticles. For example in the case of silver for sphere (radius < 30 nm) the absorption cross section plays main role and scattering is very small, but as long as the radius of the sphere increases from 30 nm the nanoparticle scatters reasonable amount of light and as a result this scatting cross section starts dominating the extinction cross section. In figure 19 (b), for sphere (r = 50 nm), there are two peaks, first at 354 nm, that is because of absorption and the other at 394 nm because of scattering. In figure 19 field enhancement of electric field

is presented that is the typical two-lobe distribution corresponding to an electric dipole but this distribution of enhanced electric field becomes 4-lobs and corresponds to quadrupole mode in the case of silver sphere for radius (r = 50 nm). On the other hand, dipole resonance is dominant mode in the case of gold sphere. Figure 19 represents the effect of size on resonance peak, in this figure the nano sphere (silver or gold) is placed in water. It can be observed that the amplitude of resonance peak can be tailored by changing the type of material. As it is evident from figure 19 (a) and 19(b) that the resonance peak amplitude for same size of sphere (silver or gold) is different. To adjust this amplitude one more factor that can play key role is surrounding medium. In this present case the surrounding medium is water. Furthermore, this value of resonance peak wavelength can be used to obtain maximum value of electric field as demonstrated in figure 20, where electric field enhancement is shown for different wavelengths.

Figure 19 – Details of extinction cross section of nanosphere.

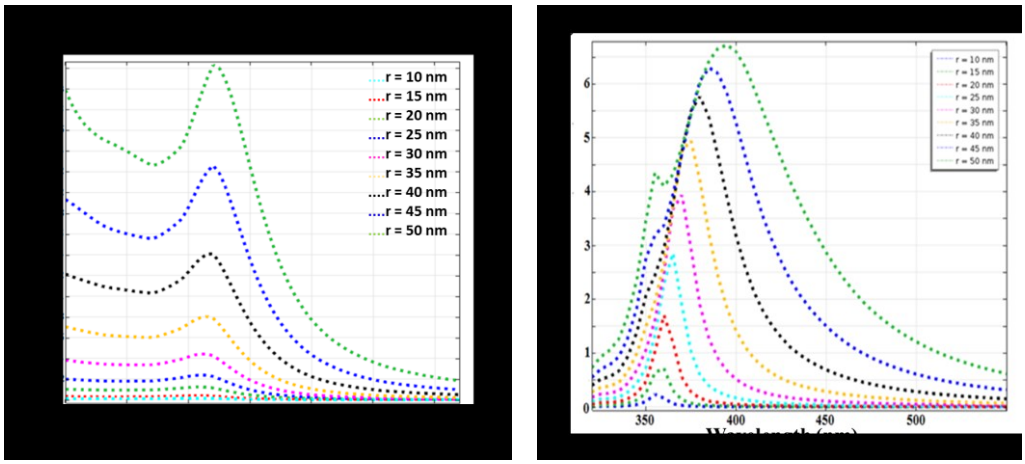

Source: The Author, 2019.

Note: (a) λ = 530 nm for gold nanosphere, (b) λ = 355 nm of silver nanosphere (radius r =10, 15, 20, 25, 30, 35, 40, 45 and 50 nm) under p-wave illumination.

One possible way to enhance electric field is to apply light with different wavelengths to obtain different values of enhanced electric field for same size of object. For example for silver or gold sphere (radius = 10 nm) we studied in figure 4.9 (a) the electric field enhancement at wavelengths ($\lambda = 450, 560, 570, 600, 660, 720,\ 530\ nm$) where 530 nm is the wavelength of resonance peak for gold sphere and in figure 4.9 (b) at wavelengths ($\lambda = 400, 450, 550, 570, 600, 660,\ 355\ nm$) where 355 nm is the wavelength of resonance peak for silver sphere.

Figure 20 - Enhancement of electric field (in V/m units) at plasmonic resonances.

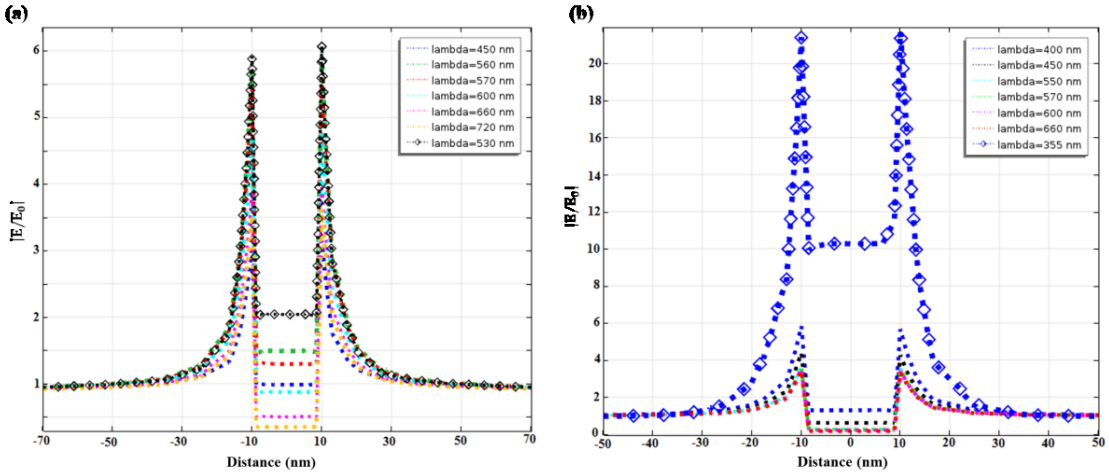

Source: The Author, 2019.

Note: (a) λ = 450, 560, 570, 600, 660 and 720 nm for gold nanosphere, (b) λ = 355, 400, 450, 550, 570, 600 and 660 nm of silver nanosphere (radius r =10 nm) under p-wave illumination.

As it is observed in figure 20 (a) and (b) that the amplitude of electric field decays exponentially as the observation point goes away from the interface. Depending on the size of nano sphere (silver or gold) the length of this field decay may vary from few nanometers upto few tens of nanometers.

4.5 Nanosphere as a nanocircuit

Equivalent circuits are very useful tool to design any object as they are scalar quantities. Being simple in nature still they are capable of capturing the properties of nanoparticles. In this section, we demonstrate how we can use optical properties to design the components of equivalent circuit. As described in, [7] impedance matching is powerful technique that can be used to design the model of any nano geometry, i.e., nanoslits [4, 55-57, 78], nanospheres [7, 23-26, 92], nanorods [84] and nanoellipsoids. [47] We assumed single silver / gold nanosphere with radius (r = 10, 15, 20, 25, 30, 35, 40, 45 and 50 nm) excited by uniform filed, as shown in figure 8 (a) with SEM images of silver and gold nanospheres in figure 8(b) and figure 8(c). The corresponding extinction cross sections (sum of scattering and absorption) is reported in figure 19. As mentioned in [7] using these measurements we can model nanocircuit that can exhibit these properties. As explained in [7], that nanocircuit can capture the resonance frequency, frequency dispersion and resonance quality factor of the measured spectra.

Figure 21 - A basic nanoscale circuit in visible regime, nanoplasmonic sphere with $\varepsilon < 0$, which provides a nanoinductor and a nanoresistor and surrounding medium that can be modeled as nanocapacitor.

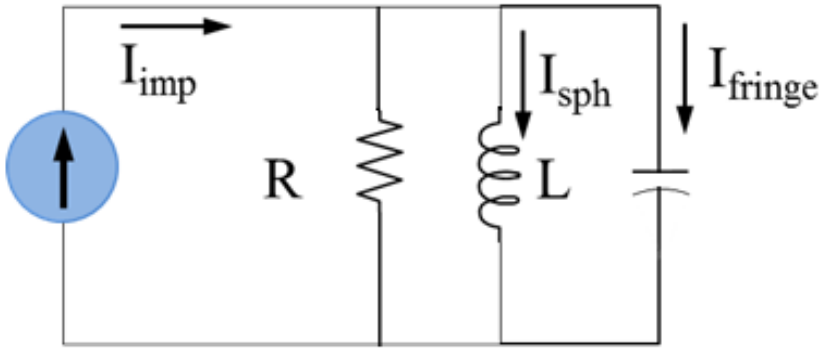

Sourece: Adopted from Ref. [7]

We consider a plasmonic nanosphere (silver or gold) with dielectric function $\varepsilon(\omega)$ that is complex quantity. The size of sphere is much smaller than the operating wavelength in the vacuum and in the plasmonic material. We consider a monochromatic incident electromagnetic plane wave illuminating the plasmonic nanosphere. The plasmonic nanosphere is placed in lossless, homogeneous, non-dispersive and isotropic media,i.e., free space. The permittivity of the free space is ε_0 and permiability is μ_0. As compare to the wavelength, the size of nanosphere is very small, so using well-known time harmonic, quasistatic approach the scattered electromagnetic fields inside of the nanosphere and in the vicinity can be calculated. [7]

Table 1 - Values of circuit elements, i.e., nano resistor, nano inductor and nano capacitor for silver sphere at corresponding wavelengths.

Radius (nm)	G_{sph}**(mS)**	L_{sph}**(femtoH)**	C_{sph}**(attoF)**	λ_0 **(nm)**
10	0.439	6.724	0.556	355
15	0.658	4.585	0.834	359
20	0.877	3.458	1.112	360
25	1.096	2.844	1.390	365
30	1.315	2.435	1.667	370
35	1.535	2.144	1.945	375
40	1.754	1.927	2.223	380
45	1.973	1.766	2.501	386
50	2.193	1.657	1.656	394

Source: The Author, 2019.

When the nanosphere is composed of a plasmonic material, such as noble metals, e.g., silver and gold, in the visible or infrared band in this case the real part of permittivity of these metals may have a negative value in these frequency bands. So the equivalent impedance of the plasmonic nanosphere can be negatively capacitive for any frequency for which $\mathrm{Re}[\varepsilon] < 0$. As discussed in [92] this can be interpreted as a positive *effective* ‘‘inductance,’’. Therefore, the equivalent circuit for the case of optical wave interaction with a plasmonic nanosphere may be presented as shown in figure 21. Depending upon the application, we can choose

current source or voltage generator. The optical circuit is driven by a current source associated with the applied fields.

Using impedance approach, we can calculate the values of capacitor, inductor and resistor as shown in table 1 by using the relations.

$$Z_{sph} = (-i\omega\varepsilon\pi \mathrm{R})^{-1} \qquad (4.6)$$

$$Z_{fringe} = (-i\omega 2\pi \mathrm{R}\varepsilon_0)^{-1} \qquad (4.7)$$

Here the equivalent circuit element for the sphere becomes:

$$L_{sph} = (-\omega^2\pi \mathrm{R}\, Re[\varepsilon])^{-1} \qquad (4.8(a))$$

$$C_{sph} = 2\pi \mathrm{R}\varepsilon_0 \qquad (4.8(b))$$

$$G_{sph} = \pi\omega \mathrm{R}\mathrm{Im}[\varepsilon] \qquad (4.8(c))$$

In this case the fringe capacitor is parallel to the inductor as a result the circuit may exhibit resonance, as mentioned in [92] this resonance corresponds to the plasmonic resonance for the metallic nanoparticles which interact with the optical wave. The resonance condition for the circuit is

$$L_{sph}C_{sph} = \omega^{-2} \qquad (4.9)$$

requires the well-known condition of plasmonic resonance for a nanosphere

$$Re\,[\varepsilon] = -2\varepsilon_0 \qquad (4.10)$$

4.6 Optical properties of ellipsoid

We will discuss the results, which have main focus on analyzing the enhanced electric field and extinction cross section of an isolated nanoellipsoid. Comparison will be made between gold particle and silver particle of the same size. The second subsection will examine the effect of the axis length distribution on the particle's optical properties. And finally based on these optical properties and using size parameters we will calculate the values of corresponding nanoelements.

In this work, for better understanding of the behavior of this quite interesting shape, in a comprehensive way the optical properties of an isolated nanoellipsoidal particle for the gold and silver cases are studied, because in nanoparticle form these two materials exhibit most interesting extinction coefficient (that is sum of absorption and scattering coefficients) in the visible and near-infrared range. The results found in this work will be useful to optimize the optical properties of nanoparticles for applications such as biosensing [21] and in the plasmonic photovoltaic field. [13, 14]

We considered the field distribution for three different wavelengths. To study the resonant plasmonic modes excited on nanoellipsoid numerical simulations are performed using finite element method (FEM) with COMSOL. In this study we are addressing 3D configuration. Perfectly-matched-layer boundary conditions are used to terminate the simulation volume. Optical data from Johnson and Christy is used to model the dielectric functions of the both materials, i.e., silver and gold. [22] The results in this section are expressed in term of electric field $E[V/m]$ and extinction cross section. In the following we discuss the details of the ellipsoids composed of gold or silver and illuminated at different wavelengths.

Figure 22 - Detail of the electric field norm E(r) (in V/m units) at resonance wavelengths.

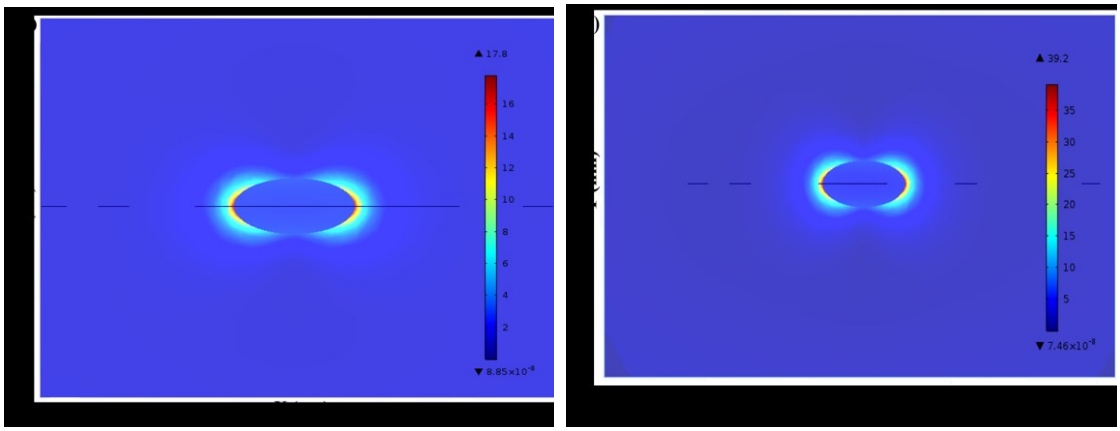

Source: The Author, 2019.

Note: (a) gold ellipsoid at λ = 450 nm and a = 50 nm (b) silver ellipsoid at λ = 570 nm and a = 50 nm.

The purpose of using same geometry for different wavelengths is to understand the behavior of nanoellipsoids composed of different materials in better way. As the field enhancement depends on the particle shape, the environment and the metal, as we mentioned in chapter 1, so one way to control this enhancement could be the coating of dielectric on ellipsoid.

In figure 22, electric field $|E/E_0|$ is shown for gold and silver sphere at resonance wavelengths. At the interface between free space and silver or gold, higher conductivities of silver and gold nanoparticles result in higher values of the field enhancement. For all wavelengths considered for both silver and gold nanoellipsoid, we observed that the electric field map shows the typical two-lobe distribution corresponding to an electric dipole oriented along the x axis of different amplitudes depending on the type of the material and corresponding wavelength. Figure 22 (a) presents the field enhancement for gold ellipsoid. The length of major axis a in this case is 50 nm. We observed in figure 22(a) that at resonance wavelength λ = 555 nm, maximum field enhancement, i.e., 17.8 times higher value of electric field near the interface between ellipsoid and free space. For same size of ellipsoid considered for silver we observe 39.2 times higher electric field enhancement as shown in figure 22 (b).

Figure 23 - Detail of the electric field norm E(r) (in V/m units) for nanoellipsoid.

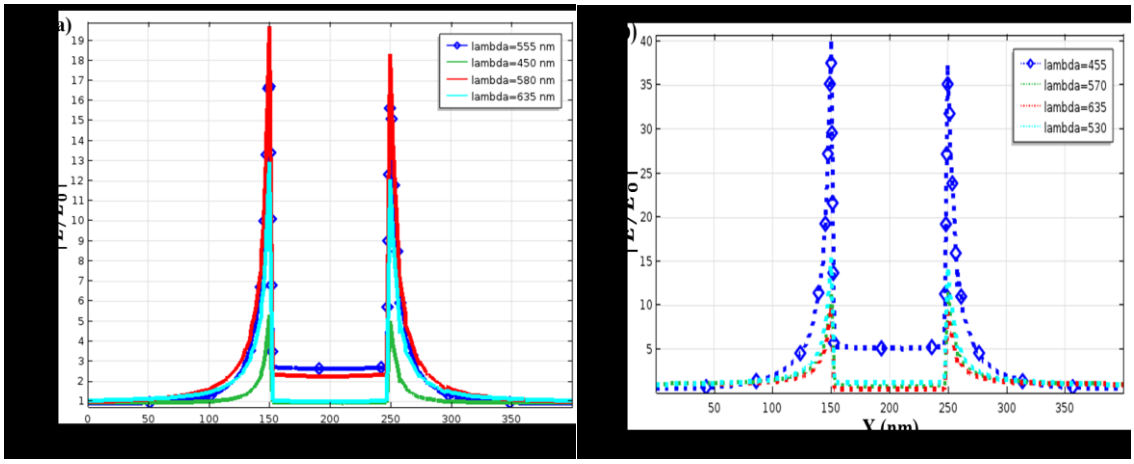

Source: The Author, 2019.

Note: (a) gold ellipsoid at λ = 450 nm, λ = 555 nm, λ = 580 nm, and λ = 635 nm and (b) silver ellipsoid at λ = 455 nm, λ = 530 nm, λ = 570 nm, and λ = 635 nm.

It is possible to change the enhanced value of electric field by changing the parameters. One possible way to do this is to apply light with different wavelengths. For example for silver or gold ellipsoids (a = 50 nm) we studied as shown in figure 23, (a) the electric field enhancement for gold ellipsoid at wavelengths ($\lambda = 450, 555, 580, 635\, nm$) we obtain maximum value of electric field at resonance peak at 555 and in figure 23 (b) at wavelengths ($\lambda = 455, 530, 570, 635\, nm$) we studied the electric field enhancement where we obtain maximum value of electric field at resonance wavelength 455 nm for silver ellipsoid.

As it is observed in figure 23 (a) and (b) that the amplitude of electric field decays exponentially as the observation point goes away from the interface. Depending on the size of

nanoellipsoid (silver or gold) the length of this field decay may vary from few nanometers upto few tens of nanometers. It is observed in figure 23 for both cases, i.e., silver and gold, especially at resonance wavelength the distribution of electric field inside the nanoellipsoid is uniform. This uniform distribution of electric field can play role in such applications where it is required to heat the nanoparticle for treatment, for example in the treatment of cancer cells it can be significant to heat these nanoparticles at resonance wavelengths.

Figure 24 - Extinction cross section of nanoellipsoid.

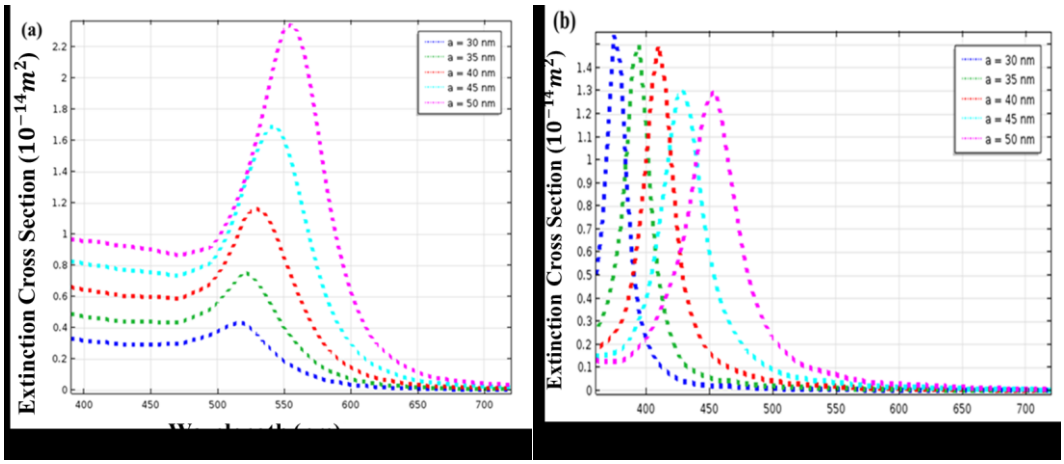

Source: The Author, 2019.

Note: (a) gold (b) silver for major axis a = 30 nm, 35 nm, 40 nm, 45 nm and 50 nm.

In figure 24, the extinction cross section of silver and gold nanoellipsoids placed in free space is presented. For silver and gold nanoellisoid, resonance peak for ellipsoid with major axis (a = 30, 35, 40, 45 and 50 nm) are observed. For both silver and gold nanoellipsoids red shift in the wavelength is observed as the length of major axis increases. For gold nanoellipsoid, the resonance peak for (a =30 nm) is at 515 nm and as the size of nanoellipsoid increases this resonance peak moves towards higher values of wavelength, i.e., for (a = 50 nm) the resonance peak is at 555 nm.

So in these 5 cases, we considered for gold nanoellipsoid we observe a red shift of 40 nm in the wavelength spectrum. For silver nanoellipsoid the resonance peak for (a = 30 nm) is at 375 nm and with increase in size of sphere the red shifted resonance peak is observed as shown in figure 24 (b), for example, for nanoellipsoid (r = 50 nm) the resonance peak is at 455 nm, showing the overall 80 nm red shift in the wavelength spectrum shown in figure 24 (b). Figure 24 represents the effect of size on resonance peak, where it is observed that the

amplitude of resonance peak can be tailored by changing the type of material and size of nanoellisoid.

Extinction cross section of small nanoparticles is the sum of scattering cross section and absorption cross section of nanoparticles. Enhanced electric field expresses the ability of the nanoellipsoid to increase the electric field at its vicinity that is dominant parameter for various applications including surface-enhanced Raman spectroscopy (SERS) or molecule sensing. On the other hand, electric field inside the nanoellipsoid is directly related to the ability of nanosphere to generate heat so the Joule effect is directly linked to the magnitude of the electric field inside the nanosellipsoid.

4.7 Optical properties of nanoprism

To study the properties of nanoprism, a series of samples of increasing edge length was prepared. The progression in color was observed as the main surface plasmon resonance is increasingly red-shifted as the nanoprism edge length increases. The SEM image of one of those sample is shown in figure 25(a) and the spectra is shown in figure 25(b). Since the spectra were obtained using UV-vis measurements of nanoprism in solution with a distribution of sizes, the spectra are inhomogeneously broadened. As shown in figure 25 (b), as the size of particle increases surface plasmon resonance is sufficiently red shifted and quadrupole SPR are more visible. The spectra of nanoprisms are highly sensitive to the size of nanprisms (figure 25(b)). The extinction coefficient of light is the net effect of absorption and scattering and explains the interaction between radiation and the material upon which is impinges. The volumetric cross-section plays a larger role in changing the spectra of silver nanoparticles as compare to the case of gold nanoparticles, indicating for a population containing equal concentrations of two sizes of silver nanoparticles, nanoparticles with larger volume contribute more to the spectra or extinction coefficient value. Similar we observed in the case of silver and gold nanospheres, in the case of nanoprisms where the extinction coefficient gets influenced by the size, the contribution of the scattering to the extinction coefficient also depends on the size of nanoparticles. As it can be seen in figure 25(b) that with increase in the size of nanoprism shoulder peak is more visible along with main resonance peak, this peak presents the scattering coefficient. This shoulder peak also describes the quadrupole nature of nanoprims. The numerical modeling of nano prisms was performed using finite element method (FEM) with COMSOL Multiphysics. Spherical perfectly-matched-layer 10 times greater than the altitude length D of nanoprism was used to

enclose the simulation volume and to avoid unnecessary reflections further proper boundary conditions were applied to study the nature of nanoprism. Optical data from Johnson and Christy [22] was used to model the dielectric functions of silver. The magnitude of the background electric field was set 1V/m.

Figure 25 – Nanoprism and its extinction cross section.

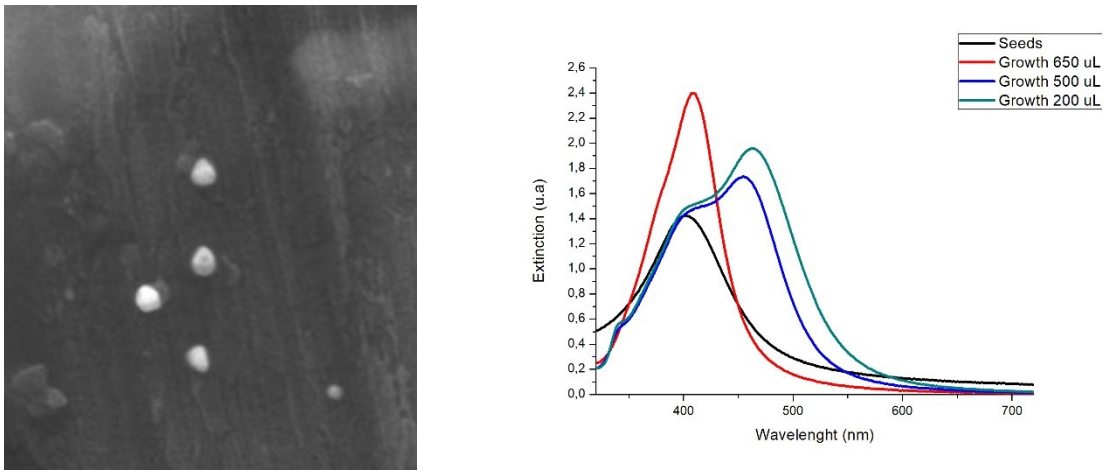

Source: The Author, 2019.

(a) Scanning electron microscopy (SEM) image of silver nanoprism with $D = 47 \pm 6$, (b) extinction cross section of nanoprism with different sizes.

Figure 26(a) displays the normalized electric field distribution ($|E/E_0|$) around a single silver nanoprism at $\lambda_0 = 635$ nm with D = 40 nm and t = 5 nm, in free space. It is evident in this figure that the field enhancement is highly localized at the corners of silver nanoprism. In this case field enhancement is 30 times higher as compare to the incident field. Where as shown in figure 26 (b) field enhancement at SPR is 300 times higher at the tip along x-direction of nanoprism much higher as compare to figure 26 (a), as shown in figure 26 (b). For dipole plasmon mode (565 nm), the strong field distributions observed at the tips of the nanoprism, indicating a higher polarization charges distribution at sharp corners/tips. The field amplitude decays exponentially as a function of distance from the nanoprism tips as shown in figure 26 (b). In figure 26 (a) and figure 26 (b), the amount of electric field is higher and approximately uniform inside the prism. This enhanced electric field inside the nanoprism has significance that is can produce heat inside of the nanoprism, so this kind of nanoparticles can be used to kill cancer cells.

Figure 26 - Electric field enhancement for nanoprism placed in free space.

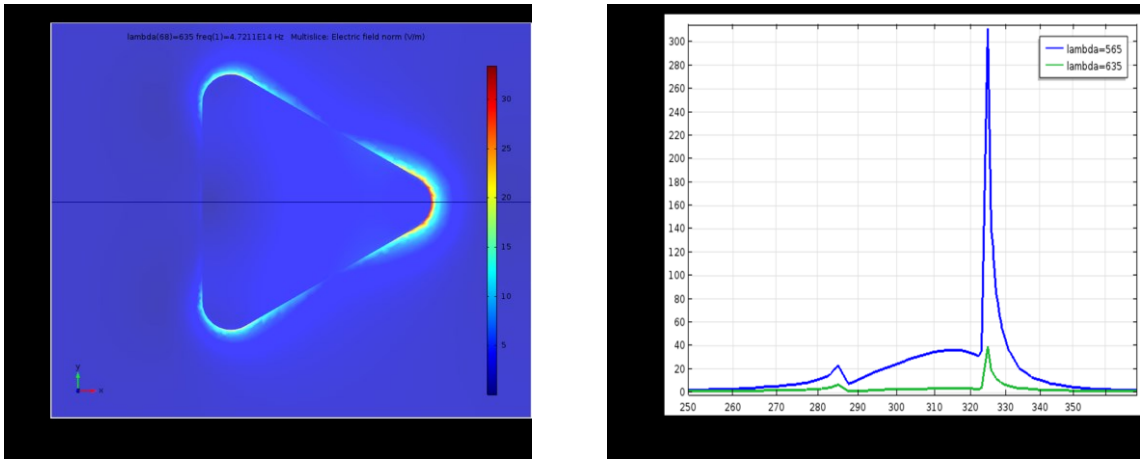

Source: The Author, 2019.

Note: (a) Electric field enhancement at resonance wavelength, (b) electric field enhancement at two different wavelengths.

Figure 27 - Extinction cross section of nanoprism.

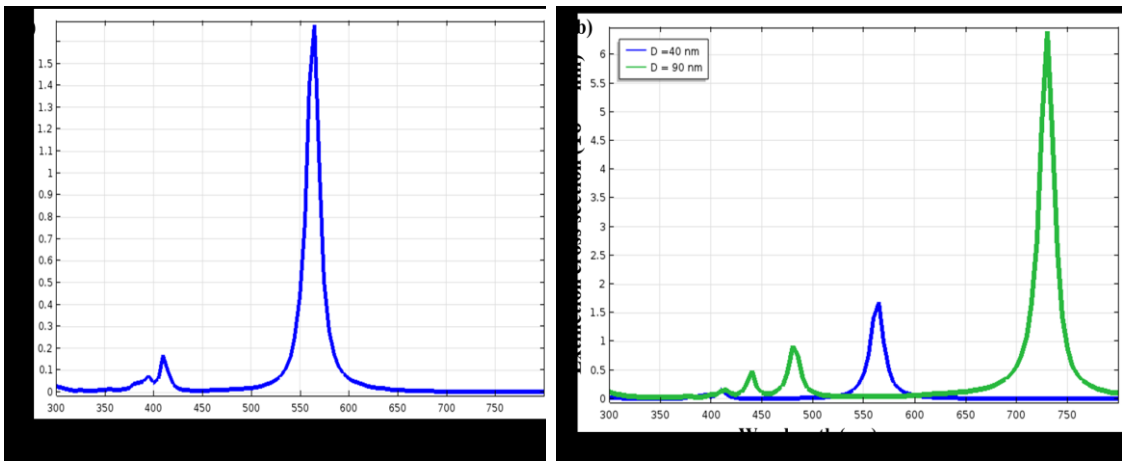

Source: The Author, 2019.

Note: (a) Extinction cross section of nanoprism with D = 40 nm, (b) comparison of extinction cross section of two nanoprisms with D = 40 nm and D = 90 nm, respectively.

In figure 27(a), the extinction cross section is shown for a nanoprism with D = 40 nm and t = 5 nm for a range of wavelength from 300 nm to 800 nm. Absorption peak is at 565 nm and the shoulder peak is at 425 nm. While keeping the thickness constant at t = 5 nm we designed a nanoprism with D = 90 nm placed in free space. In this case we observe red-shift in SPR from 565 nm to 730 nm (figure 27 (b)). The dominant mode is attributed to plasmon dipole resonance. The quadrupole peak is observed at 430 nm as shown in figure 27(b). These results in figure 27(b) indicate that with increase of size of nanoprism higher order multipole

resonances becomes visible in the extinction spectrum. In our discussion we kept the thickness of the nanoprism constant, t = 5nm. But it is possible to control the SPR of nanoprism the thickness of nanoprism can be changed to obtain required results.

5 CONCLUSIONS

In this work, we focused on designing new type of slit surrounded by two materials with different properties i.e., silver and gold. We found that for all cases considered for silver-gold nanoslit, that our newly proposed nano structure composed of silver-gold combination, can be used to obtain the intermediate values that are less than the values obtained for the case of gold and higher as compare to silver structures. In future, these interesting results will courage the researchers to apply different combinations of materials. This concept of nanoslit is like a device that can be used to control the required outputs. One may just change the material inside the slit instead of free space that we considered here and can study new problem or even it is possible to use different materials to design the nanoslit.

The other controlling possibilities are the parameters of nanoslit. As we studied (not shown in this work) that the height and width of nanoslit plays key role to enhance the parameters of incident light so one may use this option such that fulfilling the subwavelength requirement to design the parameters of slit.

In this work, we analyzed the optical properties of Au / Ag nanospheres. Based on optical properties we calculated the values of components required to design a circuit. Our circuit model is for nanospheres suspended in water whereas earlier models were considered for nanosphere placed in free space.

This work shows how one can build a circuit using optical properties of nanospheres. The values of resistor, inductor and capacitor calculated in this work are very small as compare to the values used for these components in electronics. This study suggest how one can use these nanosphere to design complex circuits for nanodevices. Silver nanospheres prepared in lab can be used as seed to prepare other complex structures. Using seed based approach we used silver nanoshperes to design silver nanoplates and we are currently using those silver nanoplates in different biological applications.

In our next work we will focus on coated spheres, ellipsoids and coated ellipsoids, as these particles can provide more options to control the functionality of nanoparticles and we will describe the relation for their nanocircuits.

A reproducible and rapid seed-based method for the preparation of silver nanoprisms in high yield is presented. The position of the main plasmon resonance and edge length of the nanoprism was readily controlled by adjusting reaction conditions. From UV-vis spectra of

solutions of the nanoprisms, the inhomogeneously broadened line width of the dipole plasmon resonance was measured and trends in the extent of plasmon resonance as a function of nanoprism size have been elucidated. Numerical simulations are performed using COMSOL Multiphysics and optical properties are discussed. The choice of selection of altitude and thickness of nanoprism can provide control on the localized surface plasmon resonance and field enhancement near the nanoprism. We found that based on optical properties, nanoprisms can be used in biomedical applications. These experimental and theoretical investigations guide towards the selection nanoprism for different applications.

REFERENCES

[1] MAIER, S. A. **Plasmonics:** fundamentals and applications. New Jersey: Springer, 2007.

[2] ZOUHDI, S.; SIHVOLA, A.; VINOGRADOV, A. P. **Metamaterials and plasmonics:** fundamentals, modelling, applications. New Jersey: Springer, 2008.

[3] BRONGERSMA, M. L.; KIK, P. G. **Surface plasmon nanophotonics**. New Jersey: Springer, 2008.

[4] WEINER, J.; NUNES, F. D. **Light-matter interaction:** physics and engineering at the nanoscale**.** Oxford: Oxford University Press, 2013.

[5] BOHREN, C. F.; HUFFMAN, D. R. **Absorption and scattering of light by small particles**. New York: Wiley, 1983.

[6] JACKSON, J. D. **Classical electrodynamics**. New York: Wiley, 1999.

[7] ENGHETA, N.; SALANDRINO, A.; ALÙ, A. Circuit elements at optical frequencies: nano-inductors, nanocapacitors and nano-resistors. **Phys. Rev. Lett.,** v. 95, p. 095504, 2005.

[8] RENDELL, R. W.; SCALAPINO, D. J. Surface plasmons confined by microstructures on tunnel junctions. **Phys. Rev. B,** v. 24, p. 3276-3294, 1981.

[9] CSURGAY, A. I.; POROD, W. Surface plasmon waves in nanoelectronic circuits. **Int. J. Circuit Theory and Applications,** v. 32, p. 339-361, 2004.

[10] GÓMEZ RIVAS, J.; JANKE, C.; BOLIVAR, P.; KURZ, H. Transmission of THz radiation through InSb gratings of subwavelength apertures. **Opt. Express,** v. 13, p. 847-859, 2005.

[11] KNEIPP, K. Single molecule detection using surface-enhanced Raman scattering. **Phys. Rev. Lett.,** v. 78, p. 1667–1670, 1997.

[12] KIM, K.; KIM, D. J.; MOON, S.; KIM, D.; BYUN, K. M. Localized surface plasmon resonance detection of layered biointeractions on metallic subwavelength nanogratings. **Nanotechnology**, v. 20, p. 315501, 2009.

[13] MAYER K. M.; HAFNER, J. H. Localized surface plasmon resonance sensors. **Chem. Rev.,** v. 111, p. 3828-3857, 2011.

[14] ALVAREZ-PUEBLA, R.; LIZ-MARZÁN, L. M.; GARCÍA DE ABAJO, F. J. Light concentration at the nanometer scale. **J. Phys. Chem. Lett.,** v. 1, p. 2428-2434, 2010.

[15] GERSTEN, J. I. Surface shape resonances**.** *In***:** CHANG, R. K.; FURTAK, T. E. (ed.**). Surface Enhanced Raman Scattering.** New York: Plenum Press, 1982. p. 89.

[16] RECHBERGER, W.; HOHENAU, A.; LEITNER, A.; KRENN, J. R.; LAMPRECHT, B.; AUSSENEGG, F. R. Optical properties of two interacting gold nanoparticles. **Opt. Comm.,** v. 220, p. 137, 2003.

[17] MOSKOVITS, M. Surface-enhanced spectroscopy. **Rev. Mod. Phys.**, v. 57, p. 783, 1985.

[18] WOKAUN, A. Surface enhancement of optical fields: mechanism and applications. **Mol. Phys.,** v. 56, p. 1, 1985.

[19] KREIBIG, U.; VOLLMER, M. **Optical properties of metal clusters.** Berlin: Springer-Verlag, 1995.

[20] KERKER, M. **The scattering of light and other electromagnetic radiation.** New York: Academic Press, 1969.

[21] JENSEN, T. R.; SCHATZ, G. C.; VAN DUYNE, R. P. Nanosphere lithography: surface plasmon resonance spectrum . . . **J. Phys. Chem. B,** v. 103, p. 2394–2401, 1999.

[22] JOHNSON, P. B.; CHRISTY, R. W. Optical constants of the noble metals. **Phys. Rev. B,** v. 6, p. 4370–4379, 1972.

[23] ENGHETA, N. Circuits with light at nanoscales: Optical nanocircuits inspired by metamaterials. **Science**, v. 317, p. 1698–1702, 2007.

[24] ALÙ, A.; YOUNG, M. E.; ENGHETA, N. Design of nanofilters for optical nanocircuits. **Physical Review B,** v. 77, p. 144107, 2008.

[25] SUN, Y.; EDWARDS, B.; ALÙ, A.; ENGHETA, N. Experimental realization of optical lumped nanocircuits at infrared wavelengths. **Nature Materials**, v. 11, p. 208–212, 2012.

[26] LIU, N.; WEN, F.; ZHAO, Y.; WANG, Y.; NORDLANDER, P.; HALAS, N. J.; ALÙ, A. Individual nanoantennas loaded with three-dimensional optical nanocircuits. **Nano Letters** v. 13, p. 142–147, 2012.

[27] MULVANEY, P. Surface plasmon spectroscopy of nanosized metal particles. **Langmuir**, v. 12, p. 788, 1996.

[28] LIZ-MARZÁ, N, L. M. Tailoring surface plasmons through the morphology and assembly of metal nanoparticles. **Langmuir,** v. 22, p.32, 2006.

[29] HAO, E.; SCHATZ, G. C. Electromagnetic fields around silver nanoparticles and dimers. **J. Chem. Phys.** v. 120, p. 357, 2004.

[30] ANGER, P.; BHARADWAJ, P.; NOVOTNY, L. Enhancement and quenching of single-molecule fluorescence. **Phys. Rev. Lett.,** v. 96, p. 113002, 2006.

[31] CHEN, Y.; MUNECHIKA, K.; GINGER, D. S. Dependence of fluorescence intensity on the spectral overlap between fluorophores and plasmon resonant single silver nanoparticles. **Nano Lett.**, v. 7, p. 690, 2007.

[32] ZHOU, X.; DONG, S. Surface enhanced Raman scattering studies on aggregated silver nanoplates in aqueous solution. **J. Phys. Chem. B**, v. 110, p. 21545, 2006.

[33] BELL, S. E. J.; SIRIMUTHU, N. M. S. Surface enhanced Raman spectroscopy (SERS) for sub-micromolar detection of DNA/RNA mononucleotides. **J. Am. Chem. Soc.** v. 128, p. 15580, 2006.

[34] KLAR, T.; PERNER, M.; GROSSE, S.; VON PLESSEN, G.; SPIRKL, W.; FELDMANN, J. Surface-plasmon resonances in single metallic nanoparticles. **Phys. Rev. Lett.** v. 80, p. 4249, 1998.

[35] MELIKYAN, A.; MINASSIAN, H. On surface plasmon damping in metallic nanoparticles. **Appl. Phys. B**, v. 78, p. 453, 2004.

[36] MUNECHIKA, K.; SMITH, J. M.; CHEN, Y.; GINGER, D. S. Surface plasmons on metal nanoparticles: the influence of shape and physical environment. **J. Phys. Chem. C**, v. 111, p. 18906, 2007.

[37] CORONADO, E. A.; SCHATZ, G. C. Surface plasmon broadening for arbitrary shape nanoparticles: a geometrical probability approach. **J. Chem. Phys.** v. 119, p. 3926, 2003.

[38] JIN, R.; CAO, Y.; MIRKIN, C. A.; KELLY, K. L.; SCHATZ, G. C.; ZHENG, J. G. Photoinduced conversion of silver nanospheres to nanoprisms. **Science,** v. 294, p. 1901, 2001.

[39] CALLEGARI, A.; TONTI, D.; CHERGUI, M. Photochemically grown silver nanoparticles with wavelength-controlled size and shape. **Nano Lett.** v. 3, p. 1565-1568, 2003.

[40] YANG, Y.; MATSUBARA, S.; XIONG, L.; HAYAKAWA, T. NOGAMI, M. Solvothermal synthesis of multiple shapes of silver nanoparticles and their SERS properties. **J. Phys. Chem. C,** v. 111, p. 9095-9104, 2007.

[41] PASTORIZA-SANTOS, I.; LIZ-MARZÁN, L. M. Synthesis of silver nanoprisms in DMF. **Nano Lett.**, v. 2, p. 903-905, 2002.

[42] LEDWITH, D. M.; WHELAN, A. M.; KELLY, J. M.; MATER, J. A rapid, straight-forward method for controlling the morphology of stable silver nanoparticles. **Chem.** v. 17, p. 2459-2464, 2007.

[43] SHUFORD, K. L.; RATNER, M. A.; SCHATZ, G. C. Multipolar excitation in triangular nanoprisms. **J. Chem. Phys.**, v. 123, p. 114713, 2005.

[44] ACHERMANN, M.; SHUFORD, K. L.; SCHATZ, G. C.; DAHANAYAKA, D. H.; BUMM, L. A.; KLIMOV, V. I. Near-field spectroscopy of surface plasmons in flat gold nanoparticles. **Opt. Lett.**, v. 32, p. 2254, 2007.

[45] NUNES, F. D.; WEINER, J. Equivalent Circuits and nanoplasmonics. **IEEE Transactions on nanotechnology**, v. 8, p. 298-302, 2009.

[46] MACCAFERRI, N.; GONZÁLEZ-DÍAZ, J. B.; BONETTI, S.; BERGER, A.; KATAJA, M.; DIJKEN, S. V.; NOGUÉS, J.; BONANNI, V.; PIRZADEH, Z.; DMITRIEV, A.; ÅKERMAN, J.; VAVASSORI, P. Polarizability and magnetoplasmonic properties of magnetic general nanoellipsoids. **Opt. Express**, v. 21, p. 9875-9889, 2013.

[47] ALÙ, A.; SALANDRINO, A.; ENGHETA, N. Coupling of optical lumped nanocircuit elements and effects of substrates. **Opt. Express**, v. 15, p. 21, 2007.

[48] GHAEMI, H. F.; THIO, T.; GRUPP, D. E.; EBBESEN, T. W.; LEZEC, H. J. Surface plasmons enhance optical transmission through subwavelength holes. **Phys. Rev. B**, v. 58, p. 6779–6782, 1998.

[49] MARTIN-MORENO, L.; GARCÍA-VIDAL, F. J.; LEZEC, H. J.; PELLERIN, K. M.; THIO, T.; PENDRY, J. B.; EBBESEN, T.W. Theory of extraordinary optical transmission through subwavelength hole arrays. **Phys. Rev. Lett.** v. 86, p. 1114–1117, 2001.

[50] BARNES, W. L.; MURRAY, W. A.; DITINGER, J.; DEVAUX, E.; EBBESEN, T. W. Surface plasmon polaritons and their role in the enhanced transmission of light through periodic arrays of subwavelength holes in a metal film. **Phys. Rev. Lett.**, v. 92, p. 107401, 2004.

[51] PORTO, J. A.; GARCIA-VIDAL, F. J.; PENDRY, J. B. Transmission resonances on metallic gratings with very narrow slits. **Phys. Rev. Lett.** v. 14, p. 83, 1999.

[52] GARCIA-VIDAL, F. J.; MARTIN-MORENO, L. Transmission and focusing of light in one-dimensional periodically nanostructured metals. **Phys. Rev. B**, v. 66, p. 155412, 2002.

[53] GARCIA-VIDAL, F. J.; LEZEC, H. J.; EBBESEN, T. W.; MARTÍN-MORENO, L. Multiple paths to enhance optical transmission through a single subwavelength slit. **Phys. Rev. Lett.** v. 90, p. 213901, 2003.

[54] TAKAKURA, Y. Optical resonance in a narrow slit in a thick metallic screen. **Phys. Rev. Lett.,** v. 24, p. 86, 2001.

[55] WEINER, J.; NUNES, F. D. High-frequency response of subwavelength-structured metals in the petahertz domain. **Opt. Express**, v. 16, p. 21256-21270, 2008.

[56] FERRI, F. A.; RIVERA, V. A. G.; OSORIO, S. P. A.; SILVA, O. B.; ZANATTA, A. R.; BORGES, B. H. V.; WEINER, J.; MAREGA, J. E. Influence of film thickness on the optical transmission through subwavelength single slits in metallic thin films. **Applied Optics**, v. 50, p. G11-G16, 2011.

[57] PARK, J. E.; TEIXEIRA, F. L.; BORGES, B. H. V. Analysis of deep-subwavelength Au and Ag slit transmittances at terahertz frequencies. **Journal of the Optical Society of America B**, v. 33, p. 1355-1364, 2016.

[58] LAL, S.; LINK, S.; HALAS, N. J. Nano-optics from sensing to waveguiding. **Nature Photonics**, v. 11, p. 641-648, 2007.

[59] DE, M.; GHOSH, P. S.; ROTELLO, V. M. Applications of nanoparticles in biology. **Advanced Materials**, v. 22, p. 4225-4241, 2008.

[60] GHOSH, R. C.; PARIA, S. Core / shell nanoparticles: classes, properties, synthesis mechanisms, characterization, and applications. **Chemical Reviews**, v. 112, p. 2373-2433, 2011.

[61] MONTEIRO, D. R.; GORUP, L. F.; TAKAMIYA, A. S.; RUVOLLO-FILHO, A. C.; DE CAMARGO, E. R.; BARBOSA, D. B.; The growing importance of materials that prevent microbial adhesion: antimicrobial effect of medical devices containing silver. **International Journal of Antimicrobial Agents**, v. 34, p. 103-110, 2009.

[62] SHARMA, V. K.; YNGARD, R. A.; LIN, Y. Silver nanoparticles: green synthesis and their antimicrobial activities. **Advanced Colloidal Interface Science**, v. 145, p. 83-96, 2009.

[63] GONG, H. M.; ZHOU, L.; SU, X. R.; XIAO, S.; LIU, S. D.; WANG, Q. Q. Illuminating dark plasmons of silver nanoantenna rings to enhance exciton–plasmon interactions. **Advanced Functional Materials**, v. 19, p. 298-303, 2009.

[64] KRUTYAKOV, Y. A.; KUDRINSKIY, A. A.; OLENIN, A. Y.; LISICHKIN, G. V. Synthesis and properties of silver nanoparticles: advances and prospects. **Russian Chemical Reviews**, v. 77, p. 233-257, 2008.

[65] KADIR, A.; Joseph, R.; Lakowiez Geddes, C. D. Rapid deposition of triangular silver nanoplates on planar surfaces: application to metal-enhanced fluorescence. **The Journal of Physical Chemistry B**, v.109, p. 6247-6251, 2005.

[66] FAHLMAN, B. D. **Materials Chemistry.** New Jersey: Springer, 2007.

[67] LI, W. R.; XIE, X. B.; SHI, Q. S.; ZENG, H. Y.; OU-YANG, Y. S.; CHEN, Y. B. Antibacterial activity and mechanism of silver nano particles on *Escherichia coli.* **Applied Microbiology and Biotechnology**, v. 85, p. 1115-22, 2010.

[68] KIMLING, J.; MAIER, M.; OKENVE, B.; KOTAIDIS, V.; BALLOT, H. PLECH, A. Turkevich method for gold nanoparticle synthesis revisited. **The Journal of Physical Chemistry B**, v. 110, p. 15700–15707, 2006.

[69] HUANG, X.; JAIN, P. K.; EL-SAYED, I. H.; EL-SAYED, M. A. Gold nanoparticles: interesting optical properties and recent applications in cancer diagnostics and therapy. **Nanomedicine**, v. 2, p. 681–693, 2007.

[70] SONNICHSEN, C.; FRANZL, T.; WILK, G. V. P. FELDMANN, J. Plasmon resonances in large noble-metal clusters. **New Journal of Physics**, v. 4, p. 93.1-93.8, 2002.

[71] JIN, R.; CAO, Y.; MIRKIN, C. A.; KELLY, K. L.; SCHATZ, G. C.; ZHENG, J. G. Photoinduced conversion of silver nanospheres to nanoprisms **Science**, v. 294, p. 1901–1903, 2001.

[72] ROTH, J. The silver anniversary of gold: 25 years of the colloidal gold marker system for immunocytochemistry and histochemistry. **Histochemistry and Cell Biology**, v. 106, p. 1–8, 1996.

[73] SZYMANSKI, H. A. **Raman Spectroscopy.** New Jersey: Springer, 1967.

[74] KLAR, T. A. **Nanophotonics with Surface Plasmons**. SHALAEV, V.; KAWATA, S. (ed.). Amsterdam: Elsevier, 2007.

[75] CSURGAY, A. I.; POROD, W. Surface plasmon waves in nanoelectronic circuits. **International Journal of Circuit Theory and Applications**, v. 32, p. 339-361, 2004.

[76] CAGLAYAN, H.; HONG, S. H.; EDWARDS, B.; KAGAN, C. R.; ENGHETA, N. Near-Infrared Metatronic Nanocircuits by Design. **Physical Review Letters**, v. 111, p. 073904, 2013.

[77] ENGHETA, N. Circuits with light at nanoscales: optical nanocircuits inspired by metamaterials. **Science**, v. 317, p. 1698–1702, 2007.

[78] NUNES, F. D.; WEINER, J. Equivalent circuits and nanoplasmonics. **IEEE Transactions on nanotechnology**, v. 8, p. 298-302, 2009.

[79] NUNES, F. D.; BORGES, B. H. V.; WEINER, J. Analysis of dispersive and dissipative media with optical resonances. **Optics Express, 20,** 15679- 15691, 2012.

[80] DAVIS, T. J.; VERNON, K. C.; GÓMEZ, D. E. Designing plasmonic systems using optical coupling between nanoparticles. **Physical Review B**, v. 79, p. 155423, 2009.

[81] ABASAHL, B.; SANTSCHI, C.; MARTIN, O. Quantitative extraction of equivalent lumped circuit elements for complex plasmonic nanostructures. **ACS Photonics**, v. 1, p. 403–407, 2014.

[82] KELLY, K. L.; CORONADO, E.; ZHAO, L. L.; SCHATZ, G. C. The optical properties of metal nanoparticles: the influence of size, shape, and dielectric environment. **J. Phys. Chem. B**, v. 107, p. 668-677, 2003.

[83] NOGUEZ, C. Surface plasmons on metal nanoparticles: the influence of shape and physical environment. **Journal of Physical Chemistry C**, v. 111, p. 3606–3619, 2007.

[84] YU, Y. Y.; CHANG, S. S.; LEE, C. L.; WANG, C. R. C. Gold nanorods: electrochemical synthesis and optical properties. **Journal of Physical Chemistry B**, v. 101, p. 6661– 6664, 1997.

[85] GRAND, J.; ADAM, P. M.; GRIMAULT, A. S. Optical extinction spectroscopy of oblate, prolate and ellipsoid shaped gold nanoparticles: experiments and theory. **Plasmonics**, v. 1, p. 135–140, 2006.

[86] GUZATOV, D. V.; KLIMOV, V. V.; PIKHOTA, M. Y. Plasmon oscillations in ellipsoid nanoparticles: beyond dipole approximation. **Laser Physics**, v. 20, p. 85–99, 2010.

[87] ALSAWAFTA, M.; WAHBEH, M.; TRUONG, V. V. Plasmonic modes and optical properties of gold and silver ellipsoidal nanoparticles by the discrete dipole approximation. **Journal of Nanomaterials**, v. 2012, p. 457968-77, 2012.

[88] FRUHNERT, M.; MONTI, A.; FERNANDEZ-CORBATON, I.; ALU, A.; TOSCANO, A.; BILOTTI, F.; ROCKSTUHL, C. Tunable scattering cancellation cloak with plasmonic ellipsoids in the visible. **Phys. Rev. B**, v. 93, p. 245127, 2016.

[89] MONTI, A.; TOSCANO, A.; BILOTTI, F. Analysis of the scattering and absorption properties of ellipsoidal nanoparticle arrays for the design of full-color transparent screens. **Journal of Applied Physics**, v. 121, p. 2431061- 2431067, 2017.

[90] GOROKHOV, V. The roots of the theoretical models of the nanotechnoscience in the electric circuit theory. **Scientific Research**, v. 2, p. 19-31, 2013.

[91] XIE, Y.; ZAKHARIAN, A. R.; MOLONEY, J. V.; MANSURIPUR, M. Transmission of light through slit apertures in metallic films. **Optics Express**, v. 12, p. 6106-6121, 2004.

[92] SHI, J; MONTICONE, F.; ELIAS, S.; WU, Y.; RATCHFORD, D.; LI, X.; ALU, A. Modular assembly of optical nanocircuits. **Nature Communications**, v. 5, p. 3896, 2014.

[93] CHAIYACHATE, P.; CHINGSUNGNOEN, A.; DASRI, T. Theoretical calculation of the optical properties of dielectric material @ noble metal core-shell composite nanoparticles. **Indian Journal of Science and Technology**, v. 10, p. 1-7, 2017.

[94] MA, Y. W.; ZHANG, J.; ZHANG, L. H.; JIAN, G. S.; WU, S. F. Theoretical analysis the optical properties of multi-coupled silver nanoshell particles. **Plasmonics**, v. 6, p. 705–713, 2011.

[95] LEVIN, C. S.; HOFMANN, C.; ALI, T. A.; KELLY, A. T.; MOROSAN, E.; NORDLANDER, P.; WHITMIRE, K. H.; HALAS, N. J. Magnetic-plasmonic core-shell nanoparticles. **ACS Nano**, v. 3, p. 1379–1388, 2009.

[96] LEE, P. C.; MELSEL, D. Adsorption and surface-enhanced Raman of dyes on silver and gold sols. **The Journal of Physical Chemistry**, v. 86, p. 3391-3395, 1982.

[97] AHERNE, D.; LEDWITH, D. M.; GARA, M.; KELLY, J. M. Optical properties and growth aspects of silver nanoprisms produced by a highly reproducible and rapid synthesis at room temperature. **Adv. Funct. Mater.** v. 18, p. 2005–2016, 2008.

APPENDIX A - Analysis of the equivalent circuit

For better analysis of the equivalent circuit presented in figure 2(a), we divide the circuit into three parts, i.e., upside, middle part and down side and simplify each part step by step.

The up side of the circuit in figure 2(a) is shown in the figure A.1 (a), containing two voltage sources, V_1 and V_2, it is assumed for simplicity that each voltage source has voltage $V_g/2$, two capacitors, C_{space} and C_i, where C_{space} represents the capacitive nature of free space and C_i is capacitance representing the phenomenon, when the charges are accumulated on the edges of nanoslit and as a result these charges generate a capacitance. Ohmic losses on both sides are assumed as $R/2$, moving currents produce inductance on each side represented by $L/2$ respectively.

Figure A.1 (a) upper part of figure 2(a), (b) simplified form of figure 4(a), (c) Thevenin equivalent circuit.

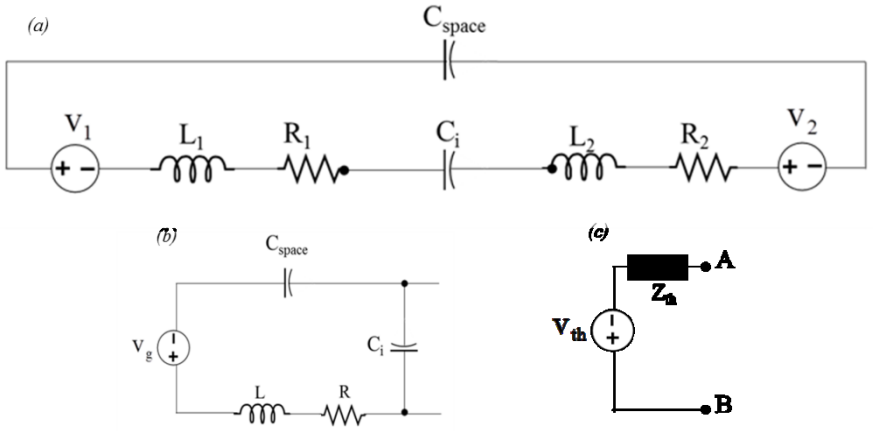

When the light interacts with the interface, then currents flow in opposite direction in both slabs and presence of charges at the edges generate displacement current respectively.

The elements of circuit shown in figure A.1 (a) can be combined as shown in figure A.1 (b) to simplify the circuit. The simplified circuit shown in figure A.1 (b) consist of a voltage source V_g, resistor R, inductor L and two capacitors C_{space} and C_i respectively. The circuit shown in figure A.1 (b) is further simplified using Thevenin theorem and finally we have Thevenin voltage followed by Thevenin resistance as presented in figure A.1(c).

$$V_{th} = \frac{\frac{1}{sC_i}}{R + sL + \frac{1}{sC_i} + \frac{1}{sC_s}} V_g = \frac{\frac{1}{LC_i}}{(s^2 + \frac{R}{L}s + (\frac{1}{LC_i} + \frac{1}{LC_s}))} V_g$$

$$V_{th} = \frac{\omega_i^2}{[s^2 + (\omega_0^2 + \omega_i^2) + \frac{R}{L}s]} V_g \quad \ldots\ldots\ldots\ldots\ldots\ldots\ldots\ldots (2.1)$$

$$Z_{th} = \frac{\frac{1}{sC_0}\left(R + sL + \frac{1}{sC_s}\right)}{\left[R + sL + \frac{1}{sC_i} + \frac{1}{sC_s}\right]}$$

After some simple calculations we find the expression for Z_{th}

$$Z_{th} = \frac{\frac{1}{sC_0}\left(s^2 + \omega_i^2 + \frac{R}{L}s\right)}{\left[s^2 + (\omega_0^2 + \omega_i^2) + \frac{R}{L}s\right]} \quad \ldots\ldots\ldots\ldots\ldots\ldots\ldots\ldots\ldots (2.2)$$

Equation (2.1) and equation (2.2) represent the Thevenin voltage and Thevenin resistance, respectively.

Figure 4 (a) represents the equivalent circuit for waveguide, that consist of two resistors R_3, R_4 and two inductors L_3, L_4, representing the resistance and inductance of both sides of waveguide, respectively. The electromagnetic details about this kind of waveguide can be seen in [12-13]. As the waveguide has a finite length and due to mismatching of impedances at both ends of the waveguide reflections occur at both ends.

Figure A.2 (a) middle part of figure 2(a), (b) reflection and transmission in waveguide.

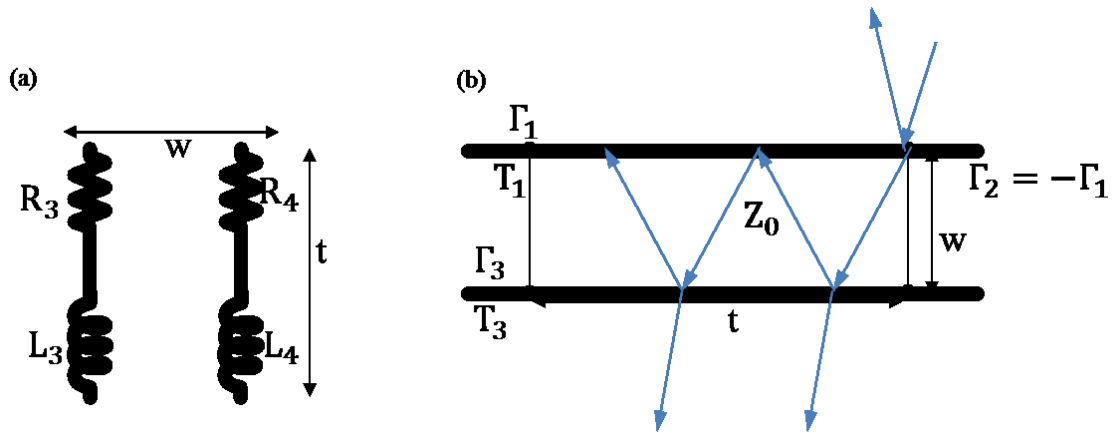

It is important to define the transmission and reflection coefficients. The reflection coefficients Γ at the interfaces are:

$$\Gamma_1 = \frac{Z_0 - Z_1}{Z_0 + Z_1} \quad \ldots\ldots\ldots\ldots\ldots\ldots\ldots\ldots\ldots\ldots\ldots\ldots\ldots\ldots (2.3)$$

$$\Gamma_2 = \frac{Z_1 - Z_0}{Z_1 + Z_0} \ldots\ldots\ldots\ldots\ldots\ldots\ldots\ldots\ldots\ldots\ldots\ldots\ldots\ldots \quad (2.4)$$

$$\Gamma_3 = \frac{Z_2 - Z_0}{Z_2 + Z_0} \ldots\ldots\ldots\ldots\ldots\ldots\ldots\ldots\ldots\ldots\ldots\ldots\ldots\ldots \quad (2.5)$$

Where Z_0, Z and Z_2 are the impedances shown in figure 2(b). Reflection coefficients Γ are related to transmission coefficients T as:

$$T_1 = 1 + \Gamma_1 \ldots\ldots\ldots\ldots\ldots\ldots\ldots\ldots\ldots\ldots\ldots\ldots\ldots\ldots \quad (2.6)$$

$$T_3 = 1 + \Gamma_3 \ldots\ldots\ldots\ldots\ldots\ldots\ldots\ldots\ldots\ldots\ldots\ldots\ldots\ldots \quad (2.7)$$

The voltage at any point within the waveguide is a sum of two wave voltage components: forward and backward. Voltage at any point within the waveguide is

$$V(z) = V_+ e^{-i\beta z} + V_- e^{i\beta z} = V_+(z) + V_-(z) \ldots (2.8)$$

$$V_+(w) = T_1 T_3 e^{-i\beta L}\left[\frac{1}{1 - \Gamma_2\Gamma_3 e^{-i2\beta L}}\right] V_+(0) = T_1 T_3 e^{-i\beta L}\left[\frac{1}{1 + \Gamma_1\Gamma_3 e^{-i2\beta L}}\right] V_+(0)$$

$$T = \frac{T_1 T_3 e^{-i\beta L}}{1 + \Gamma_1\Gamma_3 e^{-i2\beta L}} \ldots\ldots\ldots\ldots\ldots\ldots\ldots\ldots (2.9)$$

By using equation (2.6) and (2.7) we have

$$T = \frac{(1 + \Gamma_1)(1 + \Gamma_3) e^{-i\beta L}}{1 + \Gamma_1\Gamma_3 e^{-i2\beta L}} \ldots\ldots\ldots\ldots\ldots\ldots\ldots\ldots\ldots\ldots (2.10)$$

$$Z_2 = \frac{\frac{L}{s}\left(s^2 + \omega_s^2 + \frac{R}{L}s\right)\frac{1}{sC_0}}{\left(s^2 + \omega_s^2 + \frac{R}{L}s\right)\frac{L}{s} + \frac{1}{sC_0}}$$

$$Z_2 = \frac{\left(s^2 + \omega_s^2 + \frac{R}{L}s\right)\frac{1}{sC_0}}{\left(s^2 + \omega_s^2 + \frac{R}{L}s\right) + \frac{1}{LC_0}} \ldots\ldots\ldots \quad (2.11)$$

Figure A.3 (a) down side of figure 2(a), (b) compact circuit for figure 5(a), (c) impedance of circuit in figure 5(a).

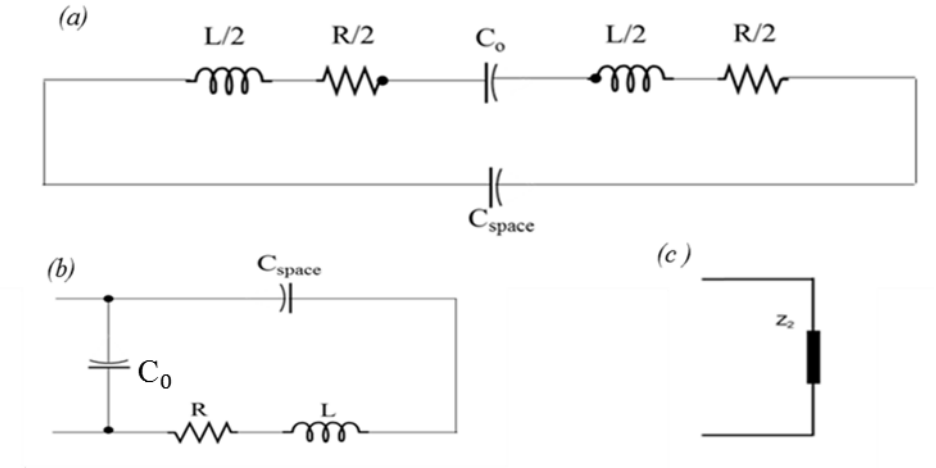

$$V_0 = \left[\frac{Z_0}{Z_{th} + Z_0}\right]\left[\left(\frac{(1+\Gamma_2)e^{-i\beta h}}{1-\Gamma_1\Gamma_2 e^{-2i\beta h}}\right)\right]V_{th} \ldots\ldots (2.12)$$

Figure A.4 impedance model of nanoslit shown in figure A. 1.

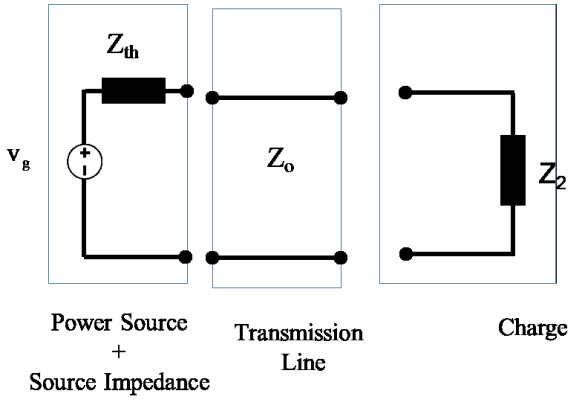

We have evaluated the core relations for source impedance and load impedance. We observe that these impedances depend upon the values of corresponding capacitance and inductance. Under certain conditions these capacitors and inductors can produce resonance.